
Break It Down: Evidence for Structural Compositionality in Neural Networks

Michael A. Lepori¹ Thomas Serre² Ellie Pavlick¹

Abstract

Many tasks can be described as compositions over subroutines. Though modern neural networks have achieved impressive performance on both vision and language tasks, we know little about the functions that they implement. One possibility is that neural networks implicitly break down complex tasks into subroutines, implement modular solutions to these subroutines, and compose them into an overall solution to a task — a property we term *structural compositionality*. Or they may simply learn to match new inputs to memorized representations, eliding task decomposition entirely. Here, we leverage model pruning techniques to investigate this question in both vision and language, across a variety of architectures, tasks, and pretraining regimens. Our results demonstrate that models oftentimes implement solutions to subroutines via modular subnetworks, which can be ablated while maintaining the functionality of other subroutines. This suggests that neural networks may be able to learn to exhibit compositionality, obviating the need for specialized symbolic mechanisms.

1. Introduction

Though neural networks have come to dominate most subfields of AI, much remains unknown about the functions that they learn to implement. In particular, there is debate over the role of *compositionality*. Compositionality has long been touted as a key property of human cognition, enabling humans to exhibit flexible and abstract language processing and visual processing, among other cognitive processes (Marcus, 2003; Piantadosi et al., 2016; Lake et al., 2017; Smolensky et al., 2022). According to common definitions (Quilty-Dunn et al., 2022; Fodor & Lepore, 2002), a rep-

resentation system is compositional if it implements a set of discrete constituent functions which exhibit some degree of modularity. That is, *blue circle* is represented compositionally if a system is able to entertain the concept *blue* independently of *circle*, and vice-versa.

It is an open question whether neural networks require explicit symbolic mechanisms to implement compositional solutions, or whether they implicitly learn compositional solutions during training. Historically, neural networks have been considered non-compositional systems, instead solving tasks by matching new inputs to memorized or “iconic” representations (Marcus, 2003; Quilty-Dunn et al., 2022). Neural networks’ apparent lack of compositionality has served as a key point in favor of integrating explicit symbolic mechanisms into artificial intelligence systems (Andreas et al., 2016; Koh et al., 2020; Ellis et al., 2020). However, modern neural networks, with no explicit inductive bias towards compositionality, have demonstrated successes on increasingly complex tasks. This raises the question: are these models succeeding by implementing compositional solutions under the hood (Mandelbaum et al., 2022)?

Contributions:

1. We introduce the concept of *structural compositionality*, which characterizes the extent to which neural networks decompose tasks into subroutines and implement them modularly. We introduce a new technique, adapted from work on model pruning, to test for structural compositionality, and apply it to several models and tasks.
2. We discover that, surprisingly, there is substantial evidence that many models implement subroutines in modular subnetworks, though most do not exhibit perfect task decomposition.
3. We characterize the effect of unsupervised pretraining on structural compositionality in fine-tuned networks and find that pretraining leads to more consistent compositional structure in language models.

¹Department of Computer Science, Brown University, Providence, RI, USA ²Carney Institute for Brain Science, Brown University, Providence, RI, USA. Correspondence to: Michael Lepori <michael.lepori@brown.edu>.

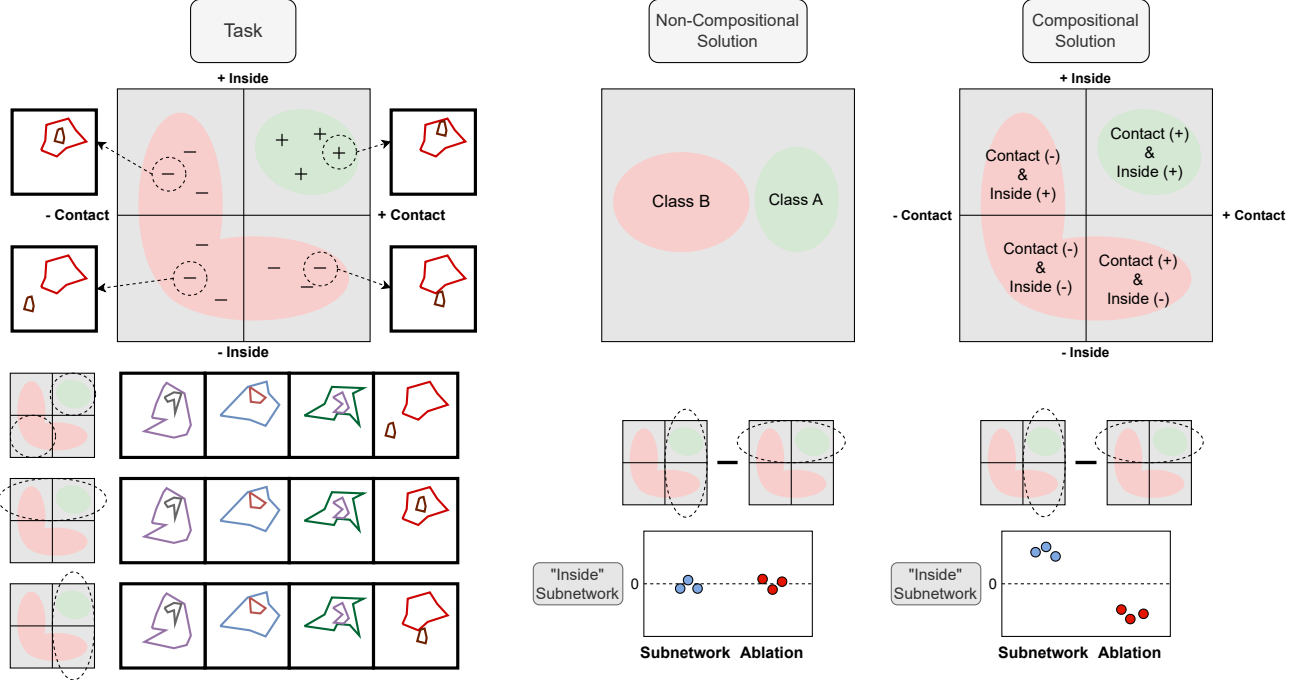


Figure 1. (Left) An illustration of the tasks used to study structural compositionality. Stimuli are generated via the composition of two subroutines: **(+/- Inside)** and **(+/- Contact)**. These stimuli are used to construct **odd-one-out** tasks, where the model is tasked with identifying the image that does not follow a rule from a set of four samples. Here, two objects must be in contact, and one must be inside the other. Rule following images correspond to the upper right quadrant. A model may solve this task in two ways. **(Middle)** It may implement a non-compositional solution, e.g., storing a prototype that encodes only the conjunction of the two subroutines. In this case, one should not be able to find a subnetwork that implements one subroutine and does not implement the other. Concretely, there should be no difference in the subnetwork’s performance on examples that depend on computing one subroutine vs. another. Ablating this subnetwork should harm the computation of both subroutines equally. In other words, neither subnetworks nor ablated models should achieve different accuracies on these two types of examples. **(Right)** A model may implement a compositional solution, which computes subroutines in modular subnetworks, and combines them. In this case, one should find a subnetwork that implements, say, **(+/- Inside)**, and this subnetwork should achieve high accuracy on examples that require computing **(+/- Inside)** and low accuracy on examples that require computing **(+/- Contact)**. In other words, the difference in accuracy between the **(+/- Inside)** and **(+/- Contact)** examples should be positive. Likewise, one should be able to ablate this subnetwork and maintain performance on **(+/- Contact)**, while compromising performance on **(+/- Inside)**, and so the difference in accuracy should be negative. Hypothetical results are represented as differences in accuracy between both types of examples.

2. Structural Compositionality

Most prior work on compositionality in neural networks has focused on whether they *generalize* in accordance with the compositional properties of data (Ettinger et al., 2018; Kim & Linzen, 2020; Hupkes et al., 2020). Such work has mostly yielded negative results—i.e., evidence that neural networks fail to generalize compositionally. This work is important for understanding how current models will behave in practice. However, generalization studies alone permit only limited conclusions about how models work under the hood.

As discussed above, leading definitions of compositionality are defined in terms of a system’s representations, not its behavior. That is, definitions contrast compositional systems

(which implement modular constituents) from noncompositional systems (which might, e.g., rely on iconic representations). Poor performance on generalization studies does not differentiate these two types of systems, since even a definitionally compositional system might fail at these generalization tasks. For example, a Bayesian network that explicitly represents and composes distinct shape and color properties might nonetheless classify a *blue circle* as a *red circle* if it has a low prior for predicting the color blue and a high prior for predicting the color red.

Thus, in this work, we focus on evaluating the extent to which a model’s representations are *structured* compositionally. Consider the task described in Figure 1. In this task, a network learns to select the “odd-one-out” among

four images. Three of them follow a compositional rule (they all contain two shapes, one of which is **inside** and **in contact** with the other). One of them breaks this rule. There are at least two ways that a network might learn to solve this type of compositional task. (1) A network might compare new inputs to prototypes or iconic representations of previously-seen inputs, avoiding any decomposition of these prototypes into constituent parts (i.e. it might implement a *non-compositional solution*). (2) A network might implicitly break the task down into subroutines, implement solutions to each, and compose these results into a solution (i.e., it might implement a *compositional solution*). In this case, the subroutines consist of a **(+/- Inside)** detector and a **(+/- Contact)** detector.

If a model trained on this task exhibits *structural compositionality*, then we would expect to find a subnetwork that implements each subroutine within the parameters of that model. This subnetwork should compute one subroutine, and not the other (Figure 1, Bottom Right; “Subnetwork”), and it should be *modular* with respect to the rest of the network — it should be possible to ablate this subnetwork, harming the model’s ability to compute one subroutine while leaving the other subroutine largely intact (Figure 1, Bottom Right; “Ablation”).

However, if a model does not exhibit structural compositionality, then it has only learned the *conjunction* of the subroutines, rather than their *composition*. It should not be possible to find a subnetwork that implements one subroutine and not the other, and ablating one subnetwork should hurt accuracy on both subroutines equally (Figure 1, Bottom Center).

3. Experimental Design

3.1. Preliminaries

Here we define terms used in the rest of the paper.

Subroutine: A binary rule. The i^{th} subroutine is denoted SR_i .

Compositional Rule: A binary rule that maps input to output according to $C = SR_1 \ \& \ SR_2$, where SR_i is a subroutine. Composition rules are denoted C .

Base Model: A model that is trained to solve a task defined by a compositional rule. Denoted M_C .

Subnetwork: A subset of the parameters of a base model, which implements one subroutine. The subnetwork that implements SR_i is denoted Sub_i . This is implemented as a binary mask, m_i , over the parameters of the base model, θ , such that $Sub_i = M_{C;\theta \odot m_i}$, where \odot refers to elementwise multiplication.

Ablated Model: The complement set of parameters of a particular subnetwork. After ablating Sub_i , we denote the ablated model M_{ablate_i} .

3.2. Experimental Logic

Consider a compositional rule, C , such as the “Inside-Contact” rule described in Figures 1 and 2. The rule is composed of two subroutines, SR_1 **(+/- Inside)** and SR_2 **(+/- Contact)**.

We define an odd-one-out task on C , as described in Section 2. See Figure 1 for three demonstrative examples using the “Inside-Contact” compositional rule.

For a given architecture and compositional rule, C , we train a base model, M_C , such that M_C solves the odd-one-out task to greater than 90% accuracy¹ (Figure 2, Panel A). We wish to characterize the extent to which M_C exhibits structural compositionality. Does M_C learn only the conjunction (effectively entangling the two subroutines), or does M_C implement SR_1 and SR_2 in modular subnetworks?

To investigate this question, we will learn a binary mask m_i over the weights θ of M_C for each SR_i , resulting in a subnetwork Sub_i . Without loss of generality, assume Sub_1 computes **(+/- Inside)** and Sub_2 computes **(+/- Contact)**, and consider investigating Sub_1 . We can evaluate this subnetwork on two partitions of the training set:

1. **Test Target Subroutine:** Cases where a model must compute the target subroutine to determine the odd-one-out (e.g., cases where the odd-one-out exhibits **(- Inside, + Contact)**).
2. **Test Other Subroutine:** Cases where a model must compute the other subroutine to determine the odd-one-out (e.g., cases where the odd-one-out exhibits **(+ Inside, - Contact)**).

If M_C exhibits structural compositionality, then Sub_1 should only be able to compute the target subroutine **(+/- Inside)**, and thus it should perform better on **Test Target Subroutine** than on **Test Other Subroutine**. If M_C entangles the subroutines, then Sub_1 will implement both subroutines and will perform equally on both partitions. See Figure 2, Panel B.

To determine modularity, we ablate the Sub_1 from the base model and observe the behavior of the resulting model, M_{ablate_1} . If M_C exhibits structural compositionality, we expect the two subroutines to be modular, such that ablating Sub_1 has more impact on M_{ablate_1} ’s ability to compute

¹This threshold was selected arbitrarily, but our results do not depend on it. All models either fail or end up achieving > 99% accuracy (See Appendix A).

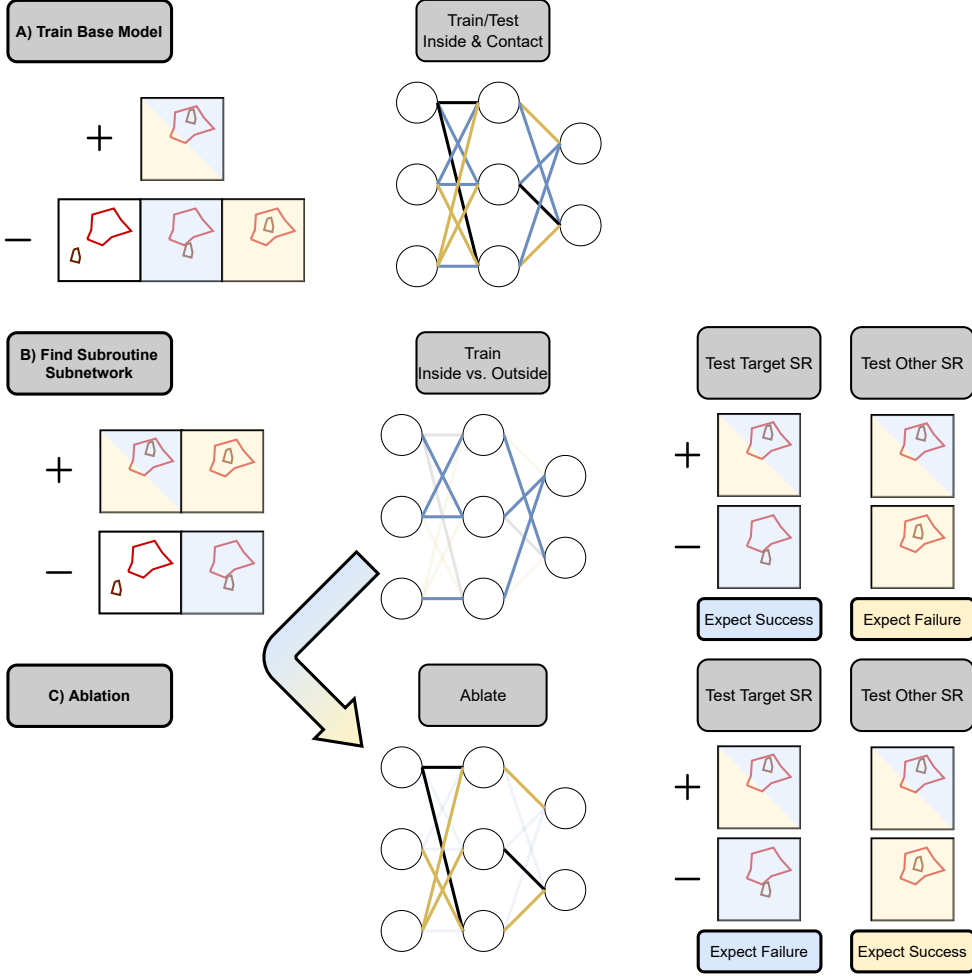


Figure 2. Illustration of the experimental design. **(A)** First, we train a neural network on a compositional task (**Inside-Contact**), ensuring that it can achieve high accuracy on the task. **(B)** We then optimize a binary mask over weights, such that the resulting subnetwork can compute one subroutine (+/- **Inside**) while ignoring the other (+/- **Contact**). We evaluate this subnetwork on datasets that require computing the target subroutine (+/- **Inside**). We also evaluate this subnetwork on datasets that require computing the other subroutine (+/- **Contact**). We expect success on the first evaluation and failure on the second if the model exhibits structural compositionality. **(C)** We invert the binary mask learned in **(B)**, ablating the subnetwork. We evaluate this on the same two datasets, expecting performance to be harmed on the target subroutine, and performance to be high for the other subroutine.

(+/- **Inside**) than (+/- **Contact**). Thus, we would expect M_{ablate_1} to perform better on **Test Other Subroutine** than **Test Target Subroutine**. See Figure 2, Panel C. However, if M_C implemented a non-compositional solution, then ablating Sub_1 should hurt performance on both partitions equally, as the two subroutines are entangled. Thus, performance on both partitions would be approximately equal.

Expected Results: For each model and task, our main results are the differences in performance between **Test Target Subroutine** and **Test Other Subroutine** for each subnetwork and ablated model. If a model exhibits structural compositionality, we expect the subnetwork to produce a positive difference in performance (**Test Target Subroutine**

Test Inside > Test Other Subroutine), and the corresponding ablated model to produce a negative difference in performance. Otherwise, we expect no differences in performance. See Figure 1 for hypothetical results.

4. Discovering Subnetworks

To discover subnetworks within our models, we use *continuous sparsification*, a model pruning technique that optimizes a deterministic binary mask over network weights to produce a subnetwork that solves a task (Savarese et al., 2020). Consider a frozen model $M_C(\cdot; w)$ trained on an odd-one-out task defined using the compositional rule C .

Within the weights of this model, we wish to discover a

subnetwork that implements SR_i ². We further require that the discovered subnetwork should be as small as possible, such that, if the model exhibits structural compositionality, it can be ablated with little damage to the remainder of the network. To encourage such sparsity, we will employ $l0$ regularization. We define the following optimization problem:

$$\min_{m_i \in \{0,1\}^d} L_{SR_i}(M_C(\cdot; w \odot m_i)) + \lambda \|m_i\|_1 \quad (1)$$

The first term describes the standard loss function given by an odd-one-out task where the rule is defined by SR_i . The second term corresponds to the $l0$ penalty, which encourages entries in the binary mask to be 0. However, optimizing such a binary mask is intractable, given the combinatorial nature of a discrete binary mask over a large parameter space. Instead, continuous sparsification reparameterizes the loss function, which allows one to optimize a mask by interpolating between a relaxed mask and a binary mask. See Appendix B for details.

5. Vision Experiments

Tasks: We extend the collection of datasets introduced in Zerroug et al. (2022), generating several tightly controlled datasets that implement compositions of the following subroutines: **contact**, **inside**, and **number**. From these three basic subroutines, we define three compositional rules: **Inside-Contact**, **Number-Contact**, and **Inside-Number**.

We will describe the **Inside-Contact** tasks in detail, as the same principles apply to the other two compositional rules (See Appendix E). This task contains four types of images, each containing two shapes. In these images, one shape is either inside and in contact with the other (**+ Inside, + Contact**), not inside of but in contact with the other (**- Inside, + Contact**), inside of but not in contact with the other (**+ Inside, - Contact**), or neither (**- Inside, - Contact**). An example in an odd-one-out task in the vision domain is defined as a collection of four images, three of which follow a rule, and one of which does not. We train our base model to solve an odd-one-out task defined by a compositional rule: images of the type (**+ Inside, + Contact**) follow the rule, and any other image type is considered the odd-one-out. See Figure 3 (Top).

In order to discover a subnetwork that implements each subroutine, we define one odd-one-out task per subroutine. To discover the **+/- Inside** Subroutine, we define (**+ Inside**) to be rule-following (irrespective of contact) and (**- Inside**) to be the odd-one-out. Similarly for the **+/- Contact** Subroutine. See Figure 3 (Middle and Bottom, respectively).

²Over all networks, we only mask weight parameters, leaving bias parameters untouched.

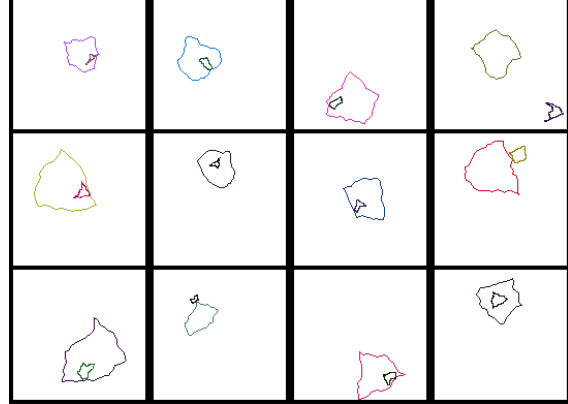


Figure 3. Three **Inside-Contact** Stimuli. The odd-one-out is always the rightmost image. (Top) An example from the task used to train the base model. (Middle) An example from the task used to discover the **+/- Inside** Subroutine. (Bottom) An example from the task used to discover the **+/- Contact** Subroutine.

The base model has only seen data where (**+ Inside, + Contact**) images are rule-following. In order to align our evaluations with the base model’s training data, we create two more datasets that probe each subroutine. For both, all rule-following images are (**+ Inside, + Contact**). To probe for (**+/- Inside**), the odd-one-out for one dataset is always a (**- Inside, + Contact**) image. This dataset is **Test Target Subroutine**, with respect to the subnetwork that implements (**+/- Inside**). Similarly, to probe for (**+/- Contact**), the odd-one-out is always a (**+ Inside, - Contact**) image. This dataset is **Test Other Subroutine**, with respect to the subnetwork that implements (**+/- Inside**).

Methods: Our models consist of a backbone followed by a 2-layer MLP³, which produces embeddings of each of the four images in an example. Following Zerroug et al. (2022) we compute the dot product between each of the four embeddings to produce a pairwise similarity metric. The least similar embedding is predicted to be the “odd-one-out”. When training a base model, our objective is the cross-entropy loss over the four images. During mask training, we append the $l0$ regularization term described in Section 4.

We investigate 3 backbone architectures: Resnet50⁴ (He et al., 2016), Wide Resnet50 (Zagoruyko & Komodakis, 2016), and ViT (Dosovitskiy et al., 2020). We perform a hyperparameter search over batch size and learning rate to find settings that allow each model to achieve near-perfect

³Hidden Size: 2048, Output Size: 128

⁴We replace all BatchNorm layers with InstanceNorm layers. BatchNorm statistics learned while training the base model do not apply to the subnetworks, and batch statistics vary across the different data partitions that we evaluate on.

performance. We then train 3 models with different random seeds, in order to probe for structural compositionality.⁵

After training our base models, M_C , we perform a hyperparameter search over continuous sparsification parameters for each subroutine (See Appendix C). One hyperparameter to note is the mask configuration: the layer of the network in which to start masking. After finding the best continuous sparsification parameters, we run the algorithm three times per model, per subroutine, and evaluate on **Test Target Subroutine** and **Test Other Subroutine**. Finally, for each subnetwork, Sub_i , we create $M_{ablate_i} = M_C - Sub_i$ and evaluate it on **Test Target Subroutine** and **Test Other Subroutine**.

6. Language Experiments

Tasks: We use a subset of the data introduced in Marvin & Linzen (2019) to construct odd-one-out tasks for language data. Analogous to the vision domain, odd-one-out tasks consist of four sentences, three of which follow a rule and one of which does not. We construct rules based on two forms of syntactic agreement: Subject-Verb Agreement and Reflexive Anaphora agreement⁶. In both cases, the agreement takes the form of a long-distance coordination of the syntactic number of two words in a sentence. First, consider the subject-verb agreement, the phenomenon that renders *the house near the fields is on fire* grammatical, and *the house near the fields are on fire* not grammatical.

Accordingly, we define the following sentence types for Subject-Verb agreement: (**{Singular/Plural} Subject, {Singular/Plural} Verb**). Because both (**Singular Subject, Singular Verb**) and (**Plural Subject, Plural Verb**) result in a grammatical sentence, we partition the Subject-Verb Agreement dataset into two subsets, one that targets singular sentences and one that targets plural sentences⁷.

For the Singular Subject-Verb Agreement dataset, base models are trained on a compositional rule that defines (**Singular Subject, Singular Verb**) sentences to be rule-following, and (**Plural Subject, Singular Verb**) and (**Singular Subject, Plural Verb**) sentences to be the odd-one-out. Thus, an example might look like this:

⁵All models are trained using the Adam optimizer (Kingma & Ba, 2014) with early stopping for a maximum of 100 epochs (patience set to 75 epochs). We evaluate using a held-out validation set after every epoch and take the model that minimizes loss on the validation set. We train without dropout, as dropout increases a model’s robustness to ablating subnetworks. We train without weight decay, as we will apply L0 regularization during mask training.

⁶Note that we are interested only in discovering some evidence of modularity within the model, rather than looking for some more profound syntactic phenomenon.

⁷See Appendix F for more details

the author in front of the ministers is short

the author the dancers love smiles

the novel that the assistants admire is good

**the picture by the ministers interest people*

All other tasks are constructed analogously to those used in the vision experiments (See Section 5). The Reflexive Anaphora dataset is constructed similarly (See Appendix F).

Methods: The language experiments proceed analogously to the vision experiments. The only difference in the procedure is that we take the representation of the [CLS] token to be the embedding of the sentence and omit the MLP. We study one architecture, BERT-Small (Bhargava et al., 2021; Turc et al., 2019), which is a BERT architecture with 4 hidden layers (Devlin et al., 2018).

7. Results

Base Model Performance: See Table 1 in Appendix A for each base model’s performance on the relevant compositional task. Most models perform near perfectly, with the exception of ViT, which failed to achieve >90% performance on any of the tasks with any configuration of hyperparameters. Thus, we exclude ViT from all subsequent analyses. This accords with ViT performance in Zerroug et al. (2022). See Appendix D for these results.

Structural Compositionality: If the base models exhibit structural compositionality, we expect subnetworks to achieve greater accuracy⁸ on **Test Target Subroutine** than on **Test Other Subroutine** (difference in accuracies > 0). After ablating subnetworks, we expect the ablated model to achieve greater accuracy on **Test Other Subroutine** than **Test Target Subroutine** (difference in accuracies < 0). Across the board, we see the expected pattern. Resnet50 and BERT results are visualized in Figure 4 (Subnetworks in Blue, Ablated Models in Red). See Appendix A for Wide Resnet50 results, which show the same trend.

For some architecture/task combinations, the pattern of results is decisively in favor of structural compositionality. See Figure 4(C, D), where all models seem to implement both subroutines in a modular fashion. Other results are mixed, such as those from Resnet50 models trained on **Number-Contact**. We see strong evidence of structural compositionality in Figure 4(E), but little evidence for it in Figure 4(F). It appears that the network is implementing the (+/- Contact) subroutine in a modular subnetwork,

⁸All accuracy values are clamped to the range [0.25, 1.0] before differences are computed. 0.25 is chance accuracy. Constraining values to this range prevents false trends from arising in the difference data due to models performing below chance.

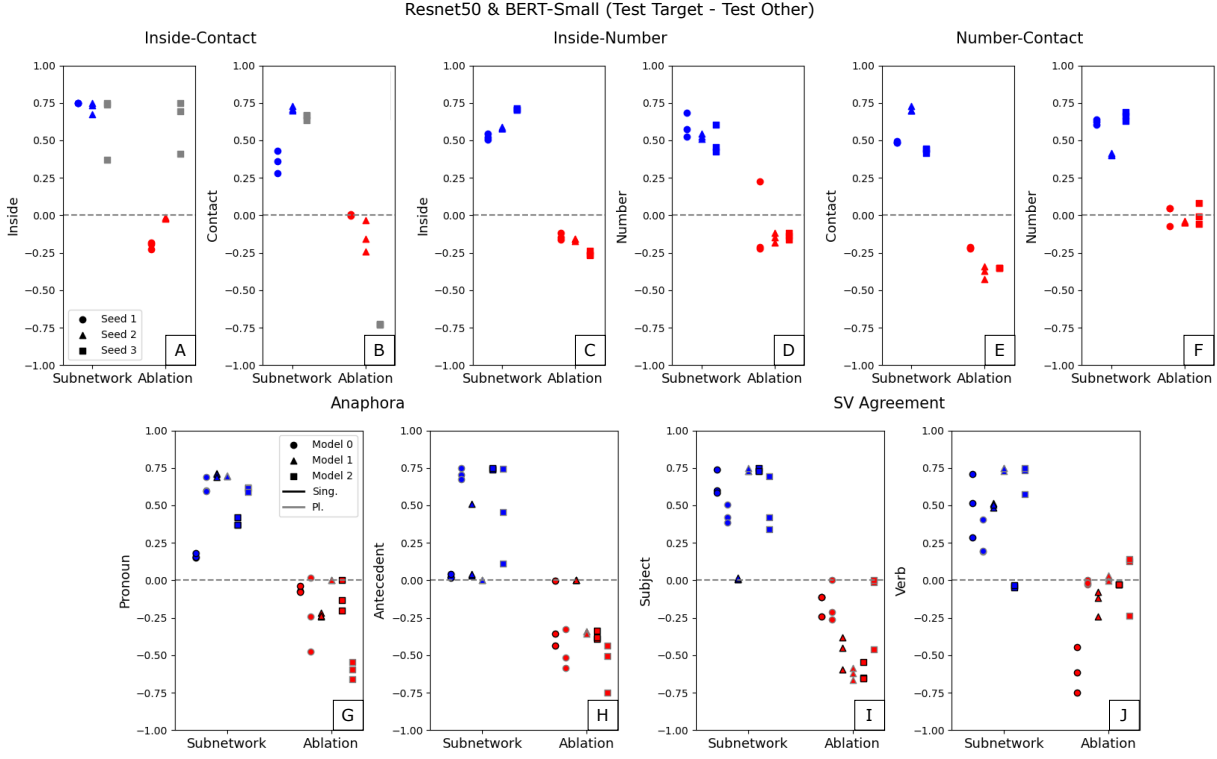


Figure 4. Results from subnetwork and ablation studies. Resnet50 results in the top row, BERT Small results in the bottom row. For each compositional task, we learn binary masks that result in subnetworks for each subroutine. Gray markers indicate that the corresponding base model did not achieve $> 90\%$ accuracy on the compositional task. **(Blue)** The difference between subnetwork performance on **Test Target Subroutine** and **Test Other Subroutine**. We expect that a subnetwork will achieve greater performance on the subroutine that it was trained to implement, resulting in values > 0 . **(Red)** After ablating the subnetwork, we evaluate on the same datasets and plot the difference again. We expect that the ablated model will achieve lower performance on **Test Target Subroutine** (which the ablated subnetwork was trained to implement), and higher performance on **Test Other Subroutine**, resulting in values < 0 .

whereas the (+/- Number) subroutine is implemented more diffusely.

8. Effect of Pretraining on Structural Compositionality

Finetuning pretrained models results in better representations and higher performance across a variety of tasks. We compare structural compositionality in models trained from scratch to those that were initialized with pretrained weights. For Resnet50, we pretrain a model on our data using SimCLR, a popular unsupervised contrastive learning algorithm (See Appendix G for more details). For BERT-Small, we use the pretrained weights provided by Turc et al. (2019). We rerun the same procedure described in Sections 5 and 6.

See Appendix A for each base model’s performance on the relevant compositional task. Figure 5 contains the results of the language experiments. Across all language tasks, the ablation results indicate that models initialized with pretrained weights reliably produce modular subnetworks. Addition-

ally, language model pretraining makes our subnetwork-discovery algorithm more stable across different random seeds. Results on vision tasks are found in Appendix A, and do not suggest any benefit of pretraining.

9. Related Work

This work casts a new lens on the study of compositionality in neural networks. Most prior work has focused on compositional generalization of standard neural models (Yu & Ettinger, 2020; Kim & Linzen, 2020; Kim et al., 2022; Dankers et al., 2022), though some has attempted to induce an inductive bias toward compositional generalization from data (Lake, 2019; Qiu et al., 2021; Zhu et al., 2021). Most closely related to the present study are prior efforts which seek to attribute causality to specific components of neural networks’ internal representations (Ravfogel et al., 2020; Bau et al., 2019; Wu et al., 2021; Tucker et al., 2021; Lovering & Pavlick, 2022). In contrast to these earlier studies, our method does not require any assumptions about where in the network the subroutine is implemented, and does not

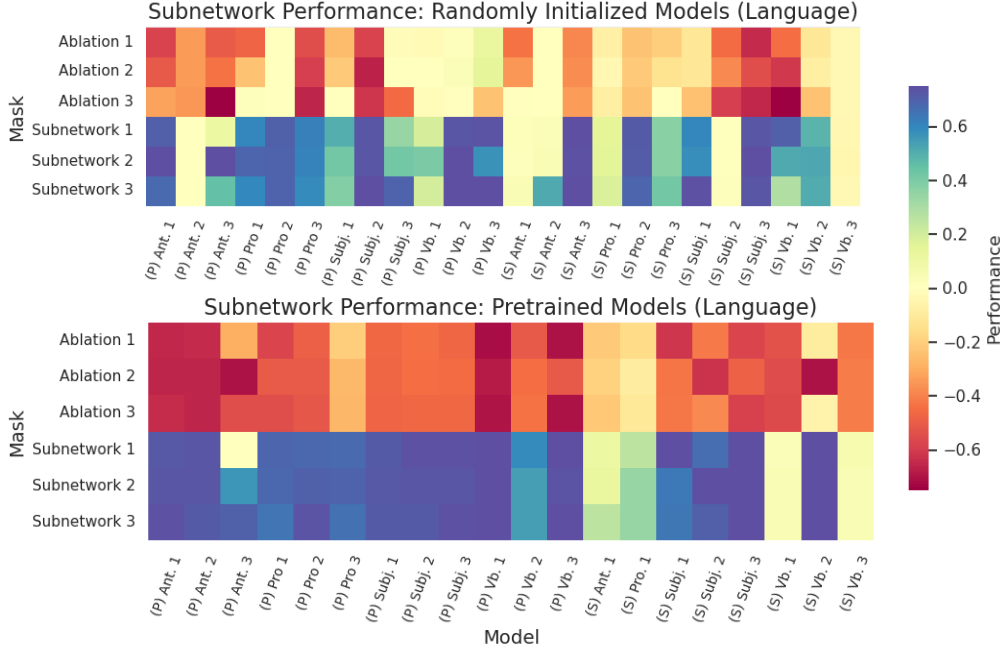


Figure 5. Performance differences between **Test Target Subroutine** and **Test Other Subroutine** for models trained from scratch and pretrained models. Across the board, we see that pretraining produces more modular subnetworks (i.e. reveal a greater disparity in performance between datasets). Base models that did not achieve >90% accuracy are omitted.

rely on auxiliary classifiers, which can confound the causal interpretation.

Our work stands adjacent to that on network pruning, which has lead to an exploration of subnetwork properties and pruning techniques (Frankle & Carbin, 2018; Paul et al., 2022; Frankle & Bau, 2019; Frankle et al., 2020; Zhou et al., 2019; Srinivas et al., 2017; Louizos et al., 2018).

More directly related to the present study is the burgeoning field of *mechanistic interpretability*, which aims to reverse engineer neural networks in order to better understand how they function (Olah, 2022). This research has led to several advancements in neural network interpretability (Elhage et al., 2022; Black et al., 2022; Henighan et al., 2023; Ganguli et al., 2021). Most related to the present study is Cammarata et al. (2020), which manually inspects individual neurons in InceptionV1 (Szegedy et al., 2015), uncovering various circuits (subnetworks) that implement various feature detectors (subroutines). Our work differs in two crucial ways: (1) We introduce a method that automatically discovers subnetworks that implement subroutines (2) Our subroutines consist of higher-level features (two shapes being inside of one another) than those in previous work (curve detectors, templates).

10. Discussion

Across a variety of architectures, tasks, and training regimens, we demonstrated that models oftentimes exhibit structural compositionality. Without any encouragement to do so, neural networks appear to decompose tasks into subtasks, and implement solutions to (at least some of) these subtasks in modular subnetworks. Furthermore, we demonstrate that self-supervised pretraining leads to more consistent structural compositionality in models finetuned on compositional tasks, at least in the domain of language.

These results bear on the longstanding debate over the need for explicit symbolic mechanisms in AI systems. Much work is focusing on integrating symbolic and neural systems (Ellis et al., 2020; Nye et al., 2020). However, our results suggest that some simple psuedo-symbolic computations might be learned directly from data using standard gradient-based optimization techniques.

These results raise several questions for future work. First, it will be important to characterize the relationship between structural compositionality and compositional generalization. Does structural compositionality impose any guarantees about a model’s generalization capabilities? Additionally, future work must clarify the relationship between pretraining and structural compositionality. Can structural compositionality be used to explain the success of large

language models? Finally, future work might seek to understand how structural compositionality arises during training — what are the dynamics that lead specific subnetworks to functionally differentiate themselves?

References

Andreas, J., Rohrbach, M., Darrell, T., and Klein, D. Neural module networks. In *Proceedings of the IEEE conference on computer vision and pattern recognition*, pp. 39–48, 2016.

Bau, A., Belinkov, Y., Sajjad, H., Durrani, N., Dalvi, F., and Glass, J. Identifying and controlling important neurons in neural machine translation. In *International Conference on Learning Representations*, 2019. URL <https://openreview.net/forum?id=H1z-PsR5KX>.

Bhargava, P., Drozd, A., and Rogers, A. Generalization in nli: Ways (not) to go beyond simple heuristics, 2021.

Black, S., Sharkey, L., Grinsztajn, L., Winsor, E., Braun, D., Merizian, J., Parker, K., Guevara, C. R., Millidge, B., Alfou, G., et al. Interpreting neural networks through the polytope lens. *arXiv preprint arXiv:2211.12312*, 2022.

Cammarata, N., Carter, S., Goh, G., Olah, C., Petrov, M., Schubert, L., Voss, C., Egan, B., and Lim, S. K. Thread: Circuits. *Distill*, 5(3):e24, 2020.

Chen, T., Kornblith, S., Norouzi, M., and Hinton, G. A simple framework for contrastive learning of visual representations. In *International conference on machine learning*, pp. 1597–1607. PMLR, 2020.

Dankers, V., Bruni, E., and Hupkes, D. The paradox of the compositionality of natural language: A neural machine translation case study. In *Proceedings of the 60th Annual Meeting of the Association for Computational Linguistics (Volume 1: Long Papers)*, pp. 4154–4175, 2022.

Devlin, J., Chang, M.-W., Lee, K., and Toutanova, K. Bert: Pre-training of deep bidirectional transformers for language understanding. *arXiv preprint arXiv:1810.04805*, 2018.

Dosovitskiy, A., Beyer, L., Kolesnikov, A., Weissenborn, D., Zhai, X., Unterthiner, T., Dehghani, M., Minderer, M., Heigold, G., Gelly, S., et al. An image is worth 16x16 words: Transformers for image recognition at scale. In *International Conference on Learning Representations*, 2020.

Elhage, N., Hume, T., Olsson, C., Schiefer, N., Henighan, T., Kravec, S., Hatfield-Dodds, Z., and Lasenby, R. Toy models of superposition. *Transformer Circuits Thread*, 2022.

Ellis, K., Wong, C., Nye, M., Sable-Meyer, M., Cary, L., Morales, L., Hewitt, L., Solar-Lezama, A., and Tenenbaum, J. B. Dreamcoder: Growing generalizable, interpretable knowledge with wake-sleep bayesian program learning. *arXiv preprint arXiv:2006.08381*, 2020.

Ettinger, A., Elgohary, A., Phillips, C., and Resnik, P. Assessing composition in sentence vector representations. In *Proceedings of the 27th International Conference on Computational Linguistics*, pp. 1790–1801, 2018.

Fodor, J. A. and Lepore, E. *The compositionality papers*. Oxford University Press, 2002.

Frankle, J. and Bau, D. Dissecting pruned neural networks. *arXiv preprint arXiv:1907.00262*, 2019.

Frankle, J. and Carbin, M. The lottery ticket hypothesis: Finding sparse, trainable neural networks. In *International Conference on Learning Representations*, 2018.

Frankle, J., Dziugaite, G. K., Roy, D., and Carbin, M. Linear mode connectivity and the lottery ticket hypothesis. In *International Conference on Machine Learning*, pp. 3259–3269. PMLR, 2020.

Ganguli, D., Hatfield-Dodds, Z., Hernandez, D., Jones, A., Kernion, J., Lovitt, L., Ndousse, K., Amodei, D., Brown, T., Clark, J., Kaplan, J., McCandlish, S., and Olan, C. A mathematical framework for transformer circuits. *Transformer Circuits Thread*, 2021.

He, K., Zhang, X., Ren, S., and Sun, J. Deep residual learning for image recognition. In *Proceedings of the IEEE conference on computer vision and pattern recognition*, pp. 770–778, 2016.

Henighan, T., Carter, S., Humne, T., Elhage, N., Lasenby, R., Fort, S., Schiefer, N., and Olah, C. Superposition, memorization, and double descent. *Transformer Circuits Thread*, 2023.

Hupkes, D., Dankers, V., Mul, M., and Bruni, E. Compositionality decomposed: How do neural networks generalise? *Journal of Artificial Intelligence Research*, 67: 757–795, 2020.

Kim, N. and Linzen, T. Cogs: A compositional generalization challenge based on semantic interpretation. In *Empirical Methods in Natural Language Processing*, 2020.

Kim, N., Linzen, T., and Smolensky, P. Uncontrolled lexical exposure leads to overestimation of compositional generalization in pretrained models. *arXiv preprint arXiv:2212.10769*, 2022.

Kingma, D. P. and Ba, J. Adam: A method for stochastic optimization. *arXiv preprint arXiv:1412.6980*, 2014.

Koh, P. W., Nguyen, T., Tang, Y. S., Mussmann, S., Pierson, E., Kim, B., and Liang, P. Concept bottleneck models. In *International Conference on Machine Learning*, pp. 5338–5348. PMLR, 2020.

Lake, B. M. Compositional generalization through meta sequence-to-sequence learning. *Advances in neural information processing systems*, 32, 2019.

Lake, B. M., Ullman, T. D., Tenenbaum, J. B., and Gershman, S. J. Building machines that learn and think like people. *Behavioral and brain sciences*, 40, 2017.

Lippe, P. Tutorial 17: Self-supervised contrastive learning with simclr. https://github.com/phlippe/uvadlc_notebooks/blob/master/docs/tutorial_notebooks/tutorial17/SimCLR.ipynb, 2022.

Louizos, C., Welling, M., and Kingma, D. P. Learning sparse neural networks through L_0 regularization. In *International Conference on Learning Representations*, 2018.

Lovering, C. and Pavlick, E. Unit testing for concepts in neural networks. *Transactions of the Association for Computational Linguistics*, 10:1193–1208, 2022.

Mandelbaum, E., Dunham, Y., Feiman, R., Firestone, C., Green, E., Harris, D., Kibbe, M. M., Kurdi, B., Mylopoulos, M., Shepherd, J., et al. Problems and mysteries of the many languages of thought. *Cognitive Science*, 46(12):e13225, 2022.

Marcus, G. F. *The algebraic mind: Integrating connectionism and cognitive science*. MIT press, 2003.

Marvin, R. and Linzen, T. Targeted syntactic evaluation of language models. *Proceedings of the Society for Computation in Linguistics (SCiL)*, pp. 373–374, 2019.

Nye, M., Solar-Lezama, A., Tenenbaum, J., and Lake, B. M. Learning compositional rules via neural program synthesis. *Advances in Neural Information Processing Systems*, 33:10832–10842, 2020.

Olah, C. Mechanistic interpretability, variables, and the importance of interpretable bases. *Transformer Circuits Thread*, 2022.

Paul, M., Chen, F., Larsen, B. W., Frankle, J., Ganguli, S., and Dziugaite, G. K. Unmasking the lottery ticket hypothesis: What’s encoded in a winning ticket’s mask? *arXiv preprint arXiv:2210.03044*, 2022.

Piantadosi, S. T., Tenenbaum, J. B., and Goodman, N. D. The logical primitives of thought: Empirical foundations for compositional cognitive models. *Psychological review*, 123(4):392, 2016.

Qiu, L., Shaw, P., Pasupat, P., Nowak, P. K., Linzen, T., Sha, F., and Toutanova, K. Improving compositional generalization with latent structure and data augmentation. *arXiv preprint arXiv:2112.07610*, 2021.

Quilty-Dunn, J., Porot, N., and Mandelbaum, E. The best game in town: The re-emergence of the language of thought hypothesis across the cognitive sciences. *Behavioral and Brain Sciences*, pp. 1–55, 2022.

Ramanujan, V., Wortsman, M., Kembhavi, A., Farhadi, A., and Rastegari, M. What’s hidden in a randomly weighted neural network? In *Proceedings of the IEEE/CVF Conference on Computer Vision and Pattern Recognition*, pp. 11893–11902, 2020.

Ravfogel, S., Elazar, Y., Gonen, H., Twiton, M., and Goldberg, Y. Null it out: Guarding protected attributes by iterative nullspace projection. In *Proceedings of the 58th Annual Meeting of the Association for Computational Linguistics*, pp. 7237–7256, 2020.

Savarese, P., Silva, H., and Maire, M. Winning the lottery with continuous sparsification. *Advances in Neural Information Processing Systems*, 33:11380–11390, 2020.

Smolensky, P., McCoy, R., Fernandez, R., Goldrick, M., and Gao, J. Neurocompositionality: From the central paradox of cognition to a new generation of ai systems. *AI Magazine*, 43(3):308–322, 2022.

Srinivas, S., Subramanya, A., and Venkatesh Babu, R. Training sparse neural networks. In *Proceedings of the IEEE conference on computer vision and pattern recognition workshops*, pp. 138–145, 2017.

Szegedy, C., Liu, W., Jia, Y., Sermanet, P., Reed, S., Anguelov, D., Erhan, D., Vanhoucke, V., and Rabinovich, A. Going deeper with convolutions. In *Proceedings of the IEEE conference on computer vision and pattern recognition*, pp. 1–9, 2015.

Tucker, M., Qian, P., and Levy, R. What if this modified that? syntactic interventions with counterfactual embeddings. In *Findings of the Association for Computational Linguistics: ACL-IJCNLP 2021*, pp. 862–875, 2021.

Turc, I., Chang, M., Lee, K., and Toutanova, K. Well-read students learn better: The impact of student initialization on knowledge distillation. *CoRR*, abs/1908.08962, 2019. URL <http://arxiv.org/abs/1908.08962>.

Wortsman, M., Ramanujan, V., Liu, R., Kembhavi, A., Rastegari, M., Yosinski, J., and Farhadi, A. Supermasks in superposition. *Advances in Neural Information Processing Systems*, 33:15173–15184, 2020.

Wu, Z., Geiger, A., Rozner, J., Kreiss, E., Lu, H., Icard, T., Potts, C., and Goodman, N. D. Causal distillation for language models. *arXiv preprint arXiv:2112.02505*, 2021.

Yu, L. and Ettinger, A. Assessing phrasal representation and composition in transformers. In *Proceedings of the 2020 Conference on Empirical Methods in Natural Language Processing (EMNLP)*, pp. 4896–4907, 2020.

Zagoruyko, S. and Komodakis, N. Wide residual networks. In *British Machine Vision Conference 2016*. British Machine Vision Association, 2016.

Zerroug, A., Vaishnav, M., Colin, J., Musslick, S., and Serre, T. A benchmark for compositional visual reasoning. In *Thirty-sixth Conference on Neural Information Processing Systems Datasets and Benchmarks Track*, 2022.

Zhou, H., Lan, J., Liu, R., and Yosinski, J. Deconstructing lottery tickets: Zeros, signs, and the supermask. *Advances in neural information processing systems*, 32, 2019.

Zhu, W., Shaw, P., Linzen, T., and Sha, F. Learning to generalize compositionally by transferring across semantic parsing tasks. *arXiv preprint arXiv:2111.05013*, 2021.

VISION	CONT.- INSIDE	CONT.- NUMBER	INSIDE- NUMBER
RN50-1	100%	99.4%	99.8%
RN50-2	100%	99.4%	99.8%
RN50-3	75.9%	99.7%	99.9%
WRN50-1	99.9%	99.6%	99.7%
WRN50-2	99.8%	99.8%	99.6%
WRN50-3	99.9%	99.4%	99.8%
LANGUAGE	SV SING.	SV PLUR.	ANAPH. SING.
BERT-SM-1	99.7%	100%	100%
BERT-SM-2	100%	100%	100%
BERT-SM-3	100%	100%	100%

Table 1. Test classification accuracy for each base model for each task. Every entry corresponds to a unique model.

VISION	CONT.- INSIDE	CONT.- NUMBER	INSIDE- NUMBER
RN50-SC-1	100%	99.7%	100%
RN50-SC-2	100%	99.6%	99.8%
RN50-SC-3	100%	99.5%	99.9%
LANGUAGE	SV SING.	SV PLUR.	ANAPH. SING.
BERT-LM-1	100%	100%	100%
BERT-LM-2	100%	100%	65.5%
BERT-LM-3	100%	100%	63.5%

Table 2. Test classification accuracy for each pretrained base model for each task. Every entry corresponds to a unique model.

A. Full Results

In this section, we provide the following results:

1. Base Model Performance on Compositional Tasks: Table 1
2. Pretrained + Finetuned Model Performance on Compositional Tasks: Table 2
3. Wide Resnet50 Subnetwork Results: Figure 6
4. Vision Pretraining vs. Random Initialization Heatmap: Figure 7
5. Absolute Accuracy for every subnetwork and ablated model on each task, for each model: Figures 8-12.

B. Continuous Sparsification: Extended Discussion

Continuous sparsification attempts to optimize a binary mask that minimizes the following loss function:

$$\min_{m_i \in \{0,1\}^d} L_{SR_i}(M_C(\cdot; w \odot m_i)) + \lambda \|m_i\|_1 \quad (2)$$

The first term describes the standard loss function given by an odd-one-out task where the rule is defined by SR_i . The second term corresponds to the l_0 penalty, which encourages entries in the binary mask to be 0. However, optimizing such a

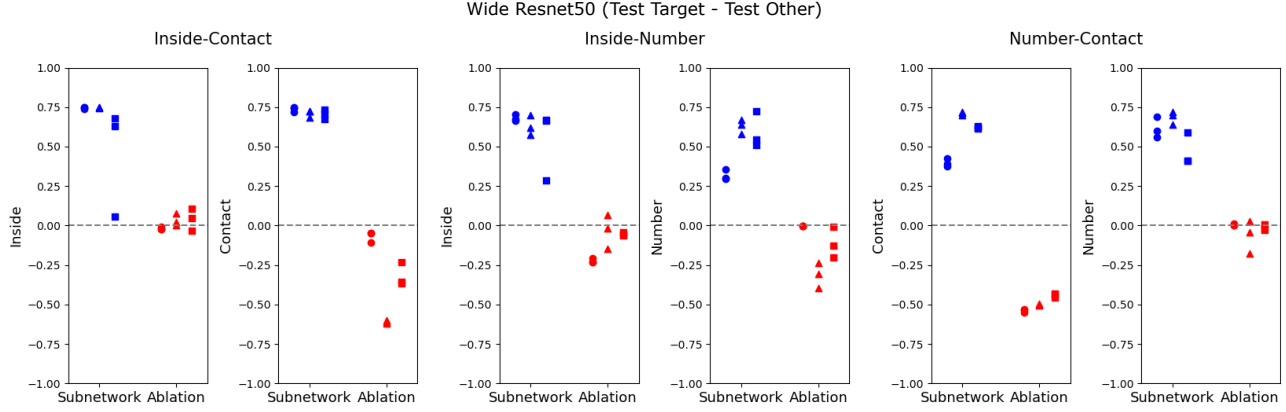


Figure 6. Wide Resnet50 subnetwork and ablation Results. Broadly, they mimic those found in Figure 4.

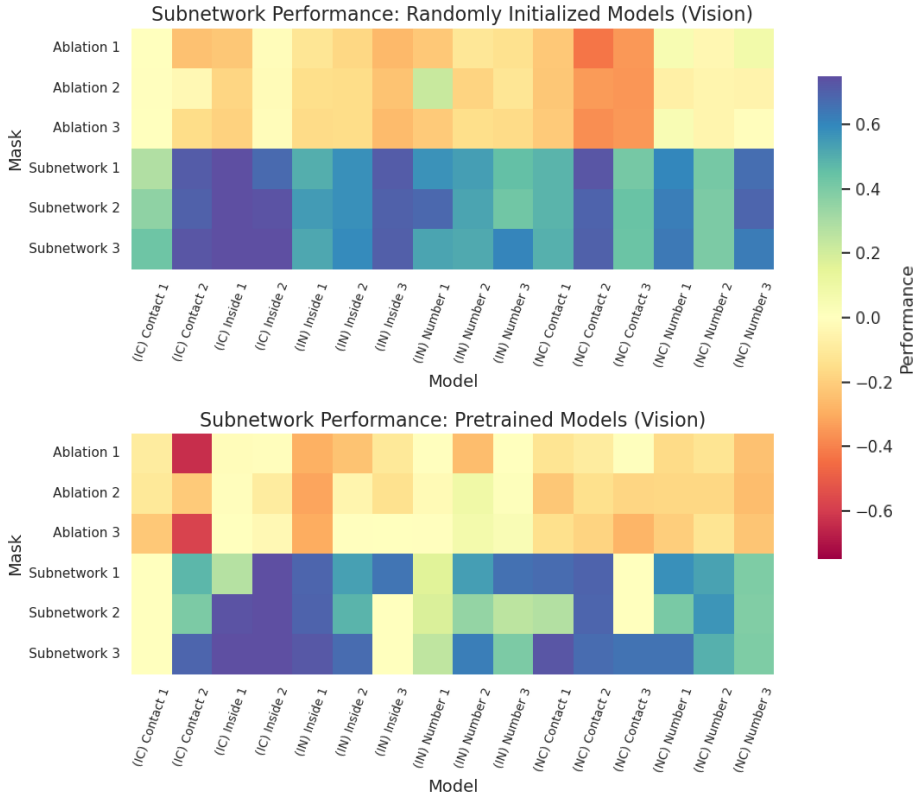


Figure 7. Vision Model Pretraining vs. Random Initialization. We observe no obvious trend differentiating the two conditions.

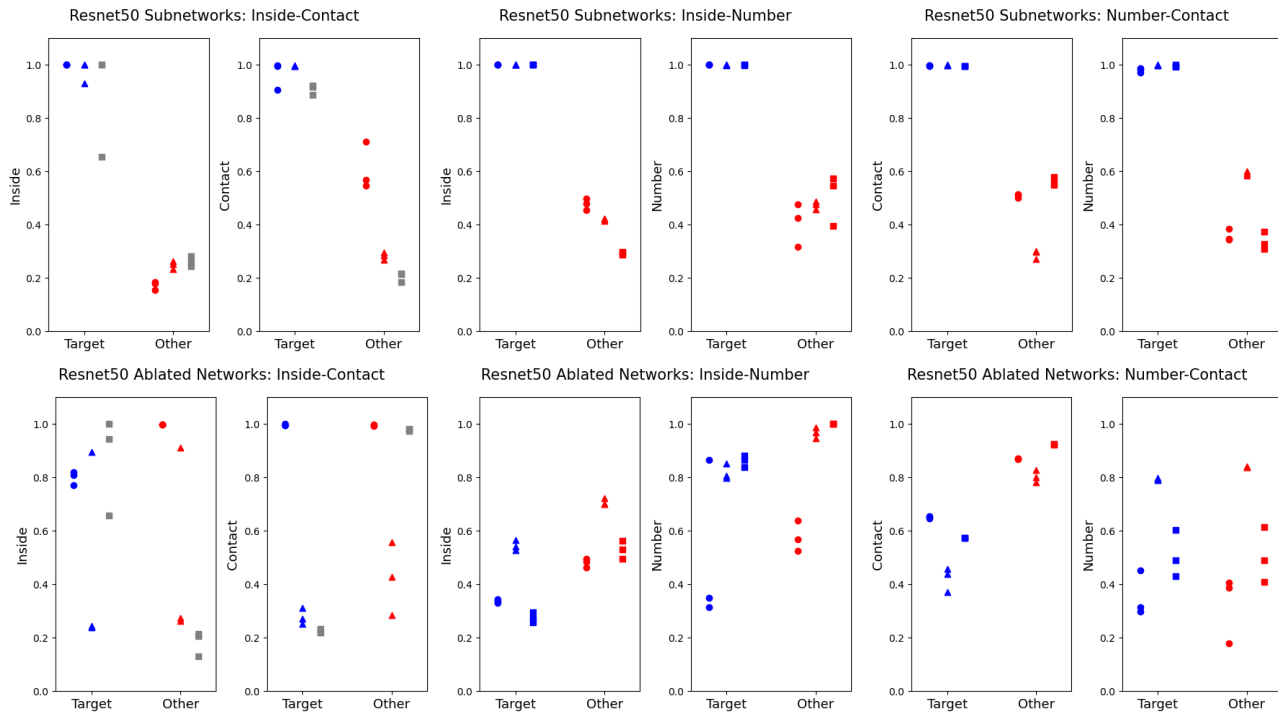


Figure 8. Resnet50 absolute performance across all conditions.

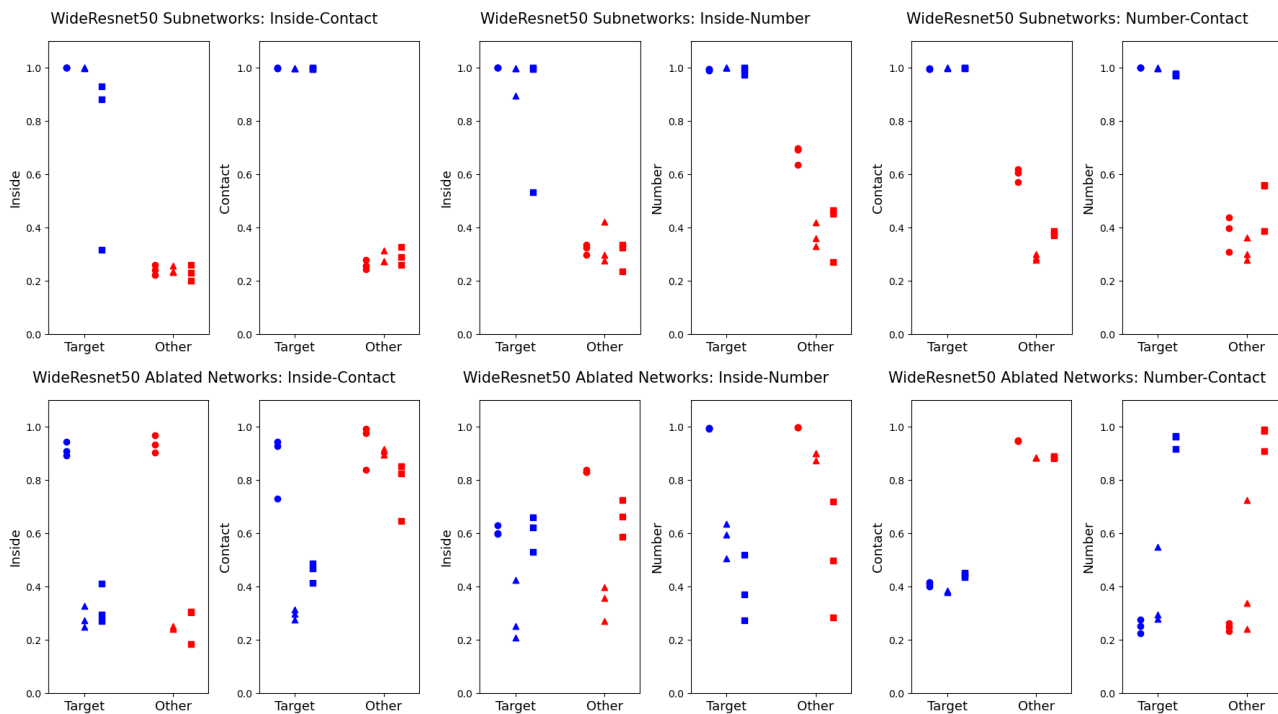


Figure 9. Wide Resnet50 absolute performance across all conditions

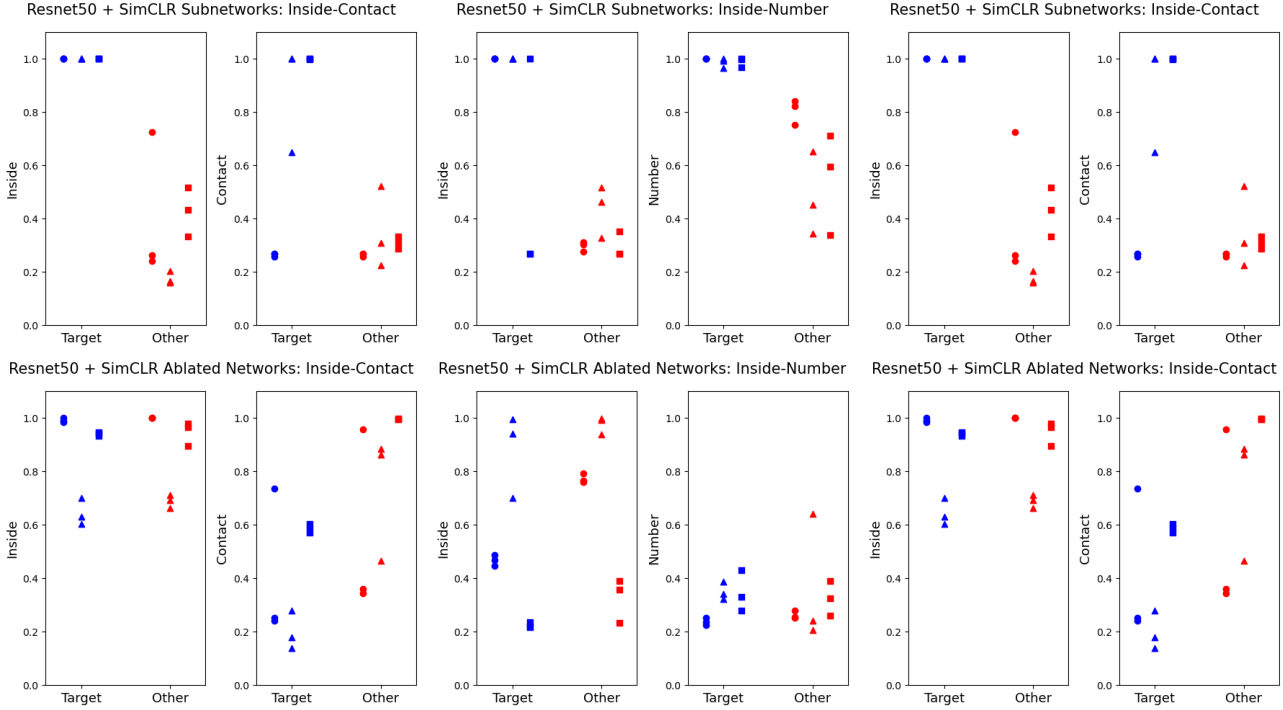


Figure 10. Resnet50 + SimCLR absolute performance across all conditions.

binary mask is intractable, given the combinatorial nature of a discrete binary mask over a large parameter space. Instead, continuous sparsification reparameterizes the loss function by introducing another variable, $s \in \mathbb{R}^d$:

$$\min_{s_i \in \mathbb{R}^d} L_{SR_i}(M_C(\cdot; w \odot \sigma(\beta \cdot s_i)) + \lambda \|\sigma(\beta \cdot s_i)\|_1) \quad (3)$$

In Equation 3, σ is the sigmoid function, applied elementwise, and β is a temperature parameter. During training β is increased after each epoch according to an exponential schedule to a large value β_{max} . Note that, as $\beta \rightarrow \infty$, $\sigma(\beta \cdot s_i) \rightarrow H(s_i)$, where $H(s_i)$ is the *heaviside function*.

$$H(s) = \begin{cases} 0, s < 0 \\ 1, s > 0 \end{cases} \quad (4)$$

Thus, during training, we interpolate between a soft mask (σ) and a discrete mask (H). During inference, we simply substitute $\sigma(\beta_{max} \cdot s_i)$ for $H(s_i)$. Notably, we apply continuous sparsification to a frozen model in an attempt to reveal the internal structure of this model, whereas the original work introduced continuous sparsification in the context of model pruning, and jointly trained w and s .

Following Savarese et al. (2020), we fix $\beta_{max} = 200$, $\lambda = 10^{-8}$, and train for 90 epochs. We train the mask parameters using the Adam optimizer with a batch size of 64 and search over learning rates.

C. Mask Hyperparameter Search Details

We search over learning rates $\{.01, .0001\}$, mask parameter initializations $\{0.1, 0.05, 0.0, -0.05\}$, and mask configurations. For Resnet models, we search over mask configurations by starting masking at different stages. We try either (1) masking the whole network, (2) beginning masking at the third (of four) stages, and (3) beginning masking at the fourth stage. For transformer models, we search over mask configurations based on layers. We try either (1) masking the whole network, (2) beginning masking at the third (of four) layers, (3) beginning masking at the fourth layer.

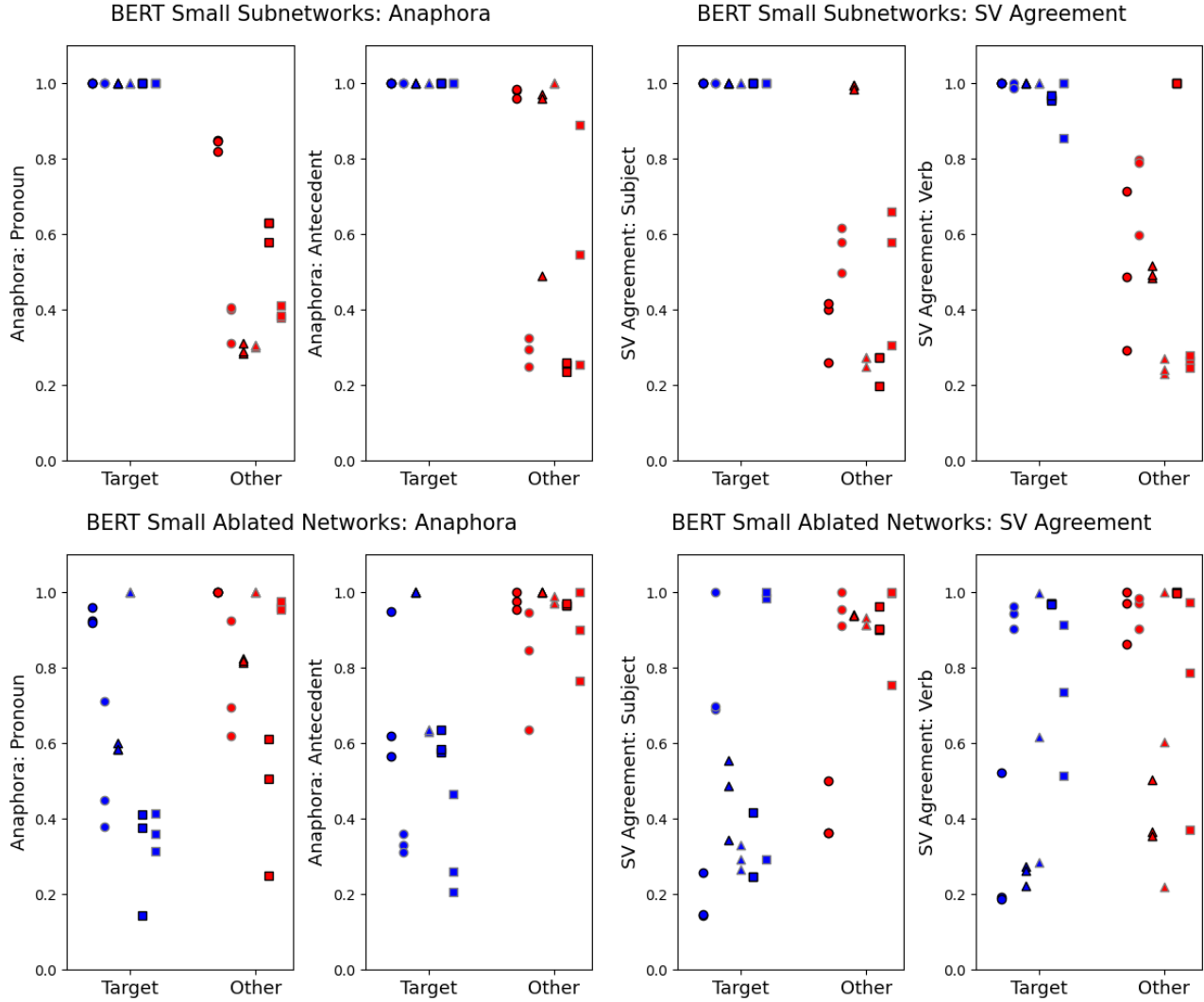


Figure 11. BERT Small absolute performance across all conditions

We perform this search independently for each trained model and each subroutine. The best hyperparameter configuration is determined based on the following criteria: The subnetwork must achieve at least 90% accuracy on the task it was trained on. This is to ensure that mask optimization succeeded. Then, it was scored on its degree of structural compositionality using the validation sets of **Test Target Subroutine** and **Test Other Subroutine**. If a subnetwork is trained to implement SR_1 , then its compositionality score is calculated using $M_{ablate_1} = M_C - Sub_1$. The score is simply the difference in accuracy that M_{ablate_1} achieves on **Test Other Subroutine** (which the ablated model should perform well on) and **Test Target Subroutine** (which the ablated model should fail on). All accuracies are clamped in the range [.25, 1], as .25 is chance accuracy. The hyperparameters that maximize this score are returned.

Note that this process is fairly computationally expensive, as it requires training many separate masks. Each mask has a parameter count comparable to its base model. Future work could improve upon the methodology presented here by reducing the number of hyperparameters that one must search over.

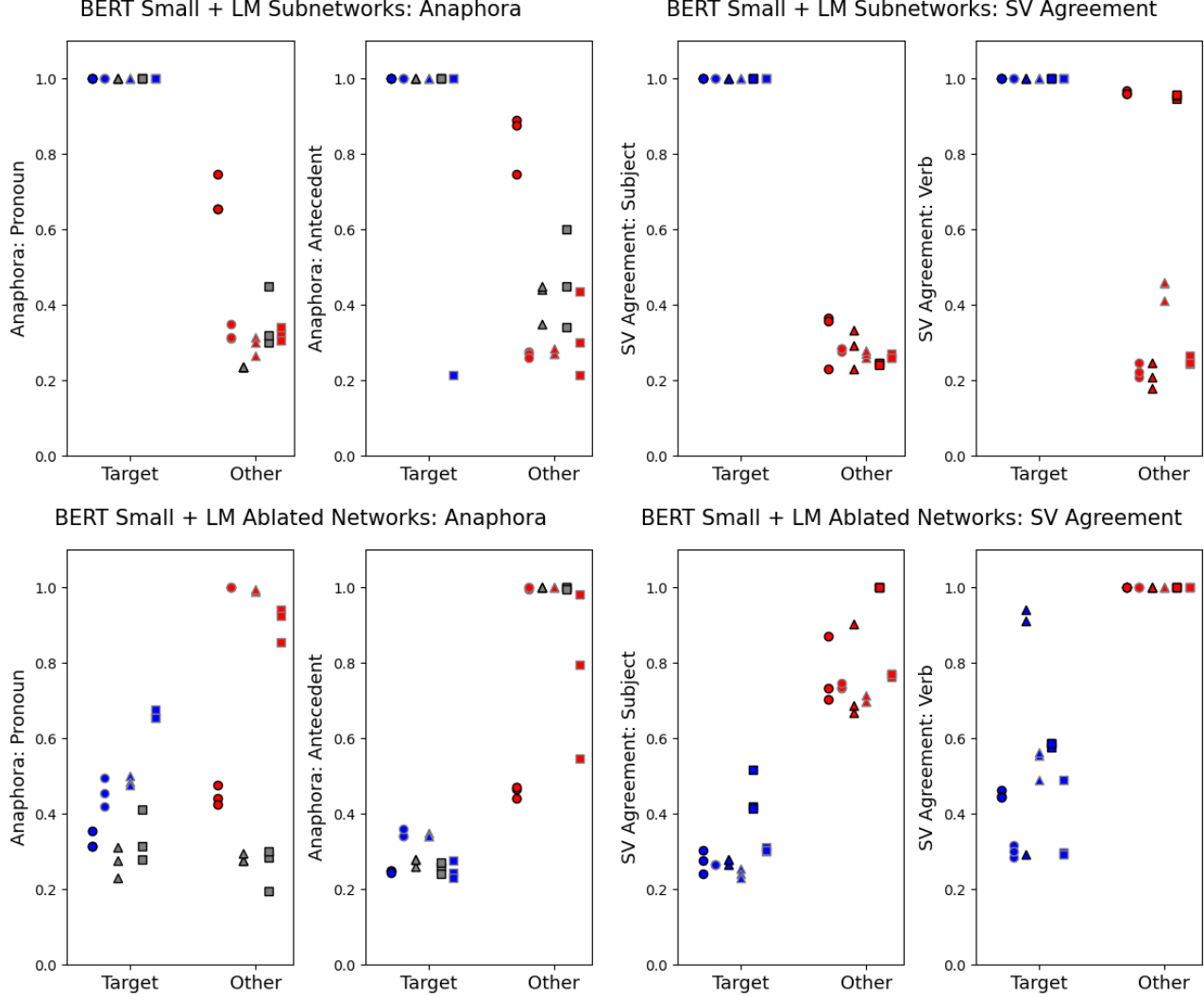


Figure 12. BERT Small + LM absolute performance across all conditions.

D. ViT Hyperparameter Search Results

See Table 3 for the results of our hyperparameter search on ViT models. We tried several batch sizes and learning rates on both a 6 and 12 layer ViT, all with a 2 layer MLP head. The MLP had a hidden layer of dimensionality 2048, and an output dimensionality of 128, similar to the Resnet50 and Wide Resnet50. Note that all models fall short of solving any of the tasks.

E. Vision Stimuli

In this section, we provide examples from all vision datasets that we use in this work. First, we describe the **+/- Number** subroutine. This subroutine operates as follows: for each training/test example, let N be an integer. All image types that exhibit **(+ Number)** will contain N shapes, whereas image types that exhibit **(- Number)** will contain M shapes, $M \neq N$. For a description of the other subroutines, refer back to Section 5.

All datasets had a training set size of 10000, a validation set size of 500, and a test set size of 1000.

# LAYERS	BATCH SIZE	LEARNING RATE	CONT.-INSIDE	CONT.-NUMBER	INSIDE-NUMBER
6	32	0.01	31%	27%	28%
6	64	0.01	28%	29%	27%
6	32	0.001	29%	27%	28%
6	64	0.001	32%	27%	26%
6	32	0.0001	25%	32%	30%
6	64	0.0001	31%	49%	32%
6	32	0.00001	42%	85%	47%
6	64	0.00001	46%	83%	54%
12	32	0.01	36%	25%	28%
12	64	0.01	27%	26%	25%
12	32	0.001	39%	31%	27%
12	64	0.001	37%	25%	22%
12	32	0.0001	41%	36%	33%
12	64	0.0001	31%	28%	31%
12	32	0.00001	40%	86%	49%
12	64	0.00001	42%	84%	51%

Table 3. Results of ViT hyperparameter search. All accuracies are rounded to the nearest % and are computed on the validation set for the relevant dataset.

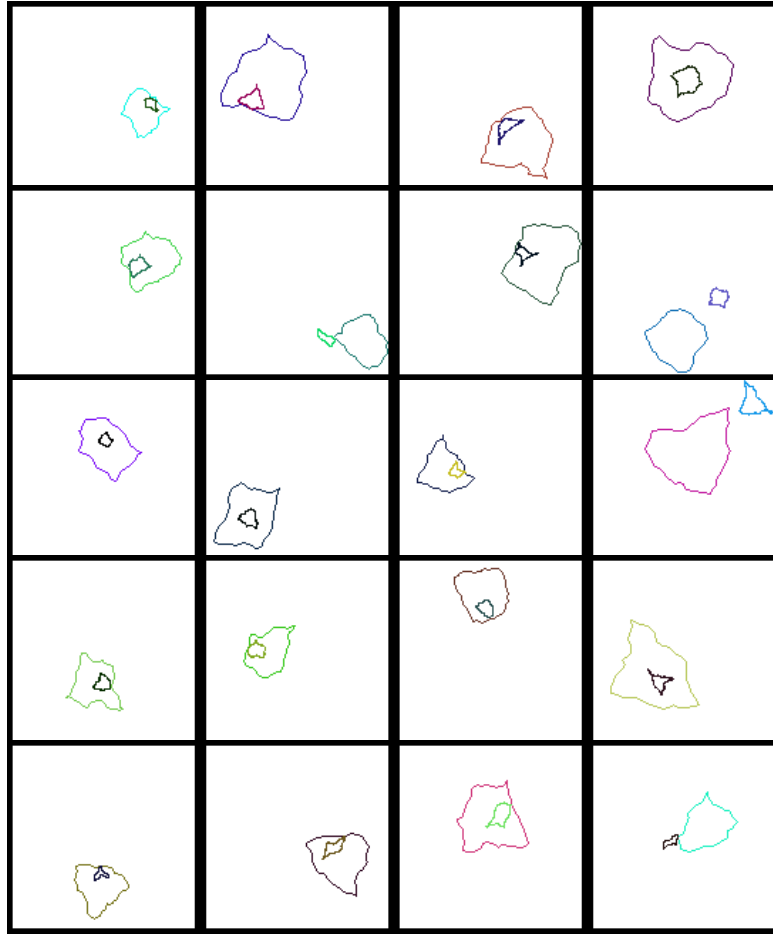


Figure 13. Examples from tasks defined over the **Inside-Contact** compositional rule. From top to bottom, we see one example from each of the following tasks: (1) The task used to train base models (2) The task used to train a **+/ Contact** subnetwork (3) The task used to train a **+/ Inside** subnetwork (4) The evaluation task used to probe for **+/ Contact** (5) The evaluation task used to probe for **+/ Inside**.

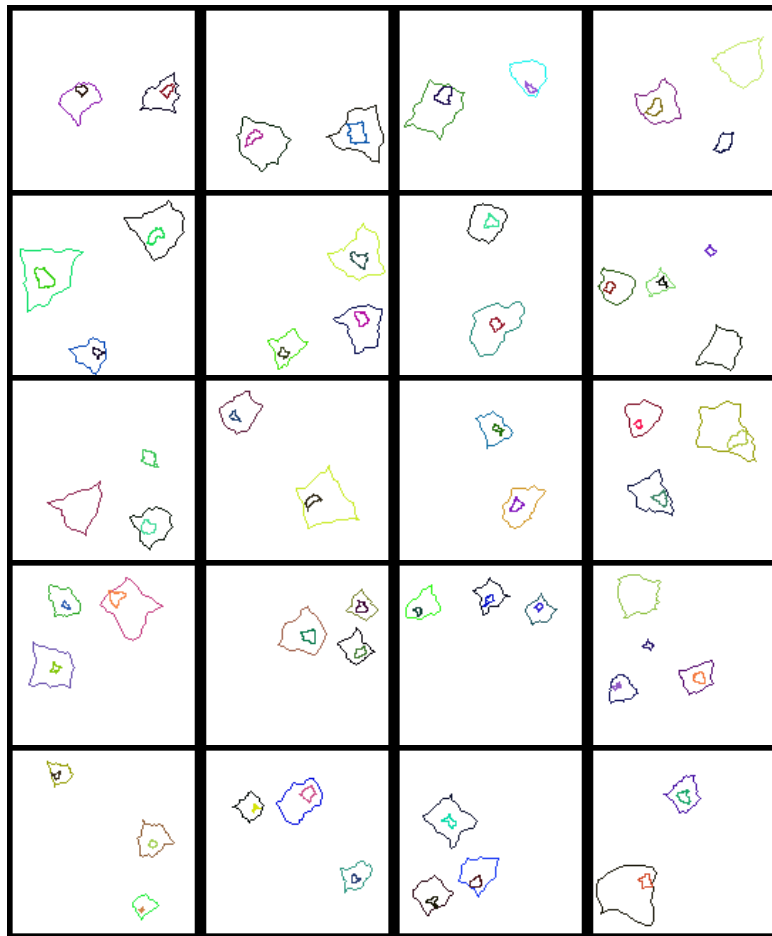


Figure 14. Examples from tasks defined over the **Inside-Number** compositional rule. From top to bottom, we see one example from each of the following tasks: (1) The task used to train base models (2) The task used to train a $+$ / $-$ **Inside** subnetwork (3) The task used to train a $+$ / $-$ **Number** subnetwork (4) The evaluation task used to probe for $+$ / $-$ **Inside** (5) The evaluation task used to probe for $+$ / $-$ **Number**.

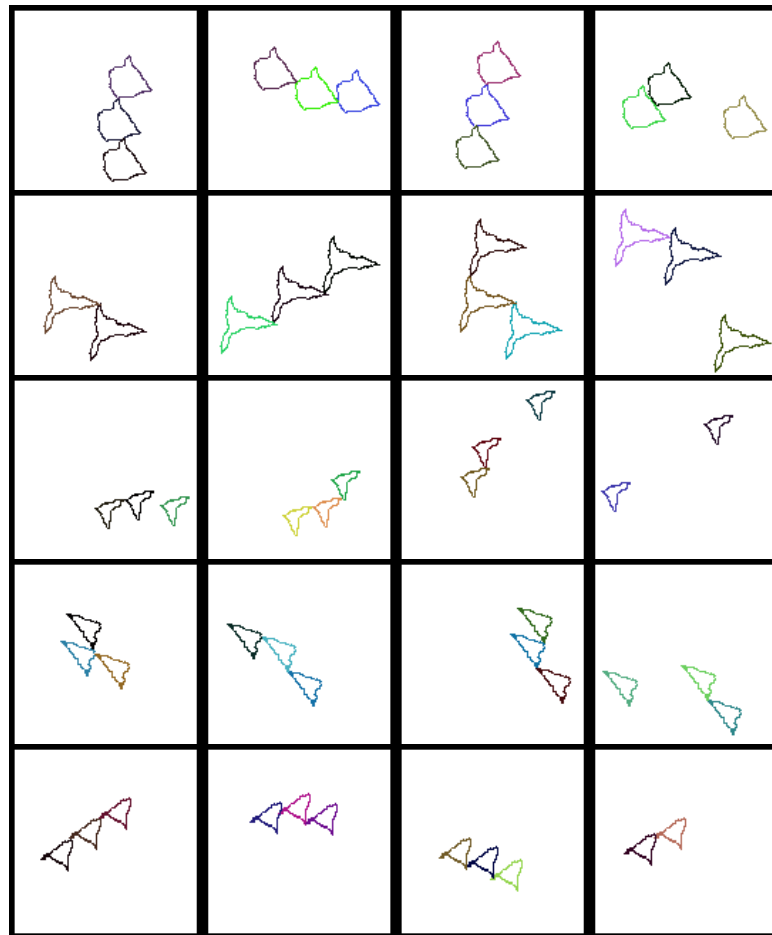


Figure 15. Examples from tasks defined over the **Number-Contact** compositional rule. From top to bottom, we see one example from each of the following tasks: (1) The task used to train base models (2) The task used to train a **+/ - Contact** subnetwork (3) The task used to train a **+/ - Number** subnetwork (4) The evaluation task used to probe for **+/ - Contact** (5) The evaluation task used to probe for **+/ - Number**.

F. Language Data Details

As noted in the main text, our language data is generated using the templates provided by [Marvin & Linzen \(2019\)](#). For the subject-verb agreement datasets, we omit templates that position the noun of interest inside either a sentential complement or an object relative clause. Thus, all of our nouns of interest are the subject of the full sentence. This is done in order to render the **(Singular/Plural Subject)** subroutine unambiguous across different sentence templates. We do the same for the Reflexive Anaphora datasets, removing the template that positions the antecedent inside a sentential complement.

These exclusions mean that the nouns of interest are always the second word of the sentence. This makes the **(Singular/Plural Subject)** subroutine amenable to a simple heuristic: check the syntactic number of the second word in the sentence, rather than first needing to identify the subject of a sentence. However, we are unconcerned about this heuristic: the present work makes no claims about how a neural network implements any *particular* subroutine, instead caring about how *several subroutines* are organized in the network’s weights (i.e. are they represented compositionally, or in an entangled fashion?).

Specifically, the subroutines we examine are those that compute the syntactic number of specific words in a sentence (either subject and verb, or antecedent and pronoun). Our goal is to find subnetworks that implement these subroutines. Consider the case of subject-verb agreement. If we were to partition our data in exactly the same way as the vision datasets, we would arrive at a compositional dataset where rule-following data points exhibit, say, **(Singular Subject, Singular Verb)**, and rule breaking examples might exhibit any of **(Plural Subject, Singular Verb)**, **(Singular Subject, Plural Verb)**, or **(Plural Subject, Plural Verb)**. However, one might expect that a pretrained network would implement syntactic number subroutines in service of another salient computation: discerning whether a sentence is grammatical or not. In this case, a pretrained model would need to unlearn this grammaticality computation, forcing two grammatical sentences apart in its embedding space. In order to avoid this potential complication, we split up our datasets into singular and plural partitions, such that only rule-following examples are grammatical (and all rule-breaking examples are ungrammatical) in each compositional dataset and subroutine test set.

Note that these datasets are smaller than those used for the vision experiments. Using the [Marvin & Linzen \(2019\)](#) templates and their provided vocabulary, and discarding the templates noted above, we arrive at the following dataset statistics (which are identical for the singular and plural instances of each dataset). For each, we provide one singular example and one plural example. The odd one out is always the fourth sentence.

- **Subject-Verb Agreement: Compositional Dataset:** 9500 (Train), 500 (Validation), 1000 (Test)

Singular

1. the farmer near the parent is old
2. the surgeon that the architects hate laughs
3. the novel that the dancer likes is new
4. the senator to the side of the parents are young

Plural

1. the farmers the taxi drivers love are short
2. the songs the dancers admire are unpopular
3. the surgeons that admire the executives are young
4. the officers that love the assistant is short

- **Subject-Verb Agreement: (Singular/Plural Subject) Dataset:** 9500 (Train), 500 (Validation), 1000 (Test)

Singular

1. the farmer that the taxi driver hates smile
2. the consultant the guards hate is young
3. the poem that the assistant likes brings joy to people
4. the customers that the chefs like is tall

Plural

1. the novels the guard hates are good
2. the teachers across from the parent is young
3. the shows that the taxi driver likes are unpopular
4. the manager across from the parent smile

- **Subject-Verb Agreement: (Singular/Plural Verb) Dataset:** 9500 (Train), 500 (Validation), 1000 (Test)

Singular

1. the game the executives admire is unpopular
2. the surgeon to the side of the taxi drivers smiles
3. the consultants the dancer likes swims
4. the painting that the chefs love are unpopular

Plural

1. the customer the assistant loves swim
2. the surgeons that the executive likes are short
3. the authors that love the chef swim
4. the officers that like the assistant swims

- **Subject-Verb Agreement: Test (Singular/Plural Subject) Dataset:** 300 (Validation), 300 (Test)

Singular

1. the teacher to the side of the taxi driver swims
2. the farmer that the chef likes is young
3. the novel the ministers admire is bad
4. the customers in front of the dancers is old

Plural

1. the pictures by the skater interest people
2. the movies the skater admires are bad
3. the pilots in front of the taxi driver are tall
4. the consultant that the dancer likes are old

- **Subject-Verb Agreement: Test (Singular/Plural Verb) Dataset:** 300 (Validation), 300 (Test)

Singular

1. the senator the taxi drivers admire is young
2. the pilot to the side of the dancer smiles
3. the farmer the assistant admires is young
4. the pilot that loves the minister are tall

Plural

1. the poems that the chefs hate are bad
2. the surgeons in front of the dancer laugh
3. the surgeons near the taxi drivers smile
4. the farmers behind the architects is short

- **Reflexive Anaphora: Compositional Dataset:** 2500 (Train), 200 (Validation), 200 (Test)

Singular

1. the consultant that the chef loves disguised himself
2. the manager that the architects hate congratulated herself
3. the pilot that the architects admire hurt herself

4. the surgeon that the executives like congratulated themselves

Plural

1. the consultants that the guards love injured themselves
2. the senators that the minister admires embarrassed themselves
3. the officers that the assistant likes embarrassed themselves
4. the teacher that the dancer loves embarrassed themselves

• **Reflexive Anaphora: (Singular/Plural Antecedent) Dataset:** 2500 (Train), 200 (Validation), 200 (Test)

Singular

1. the officer that the taxi driver likes doubted herself
2. the author that the architect loves hated himself
3. the manager that the executives love disguised herself
4. the customers that the parent likes disguised himself

Plural

1. the authors that the skater hates doubted himself
2. the surgeons that the parents admire hurt themselves
3. the officers that the taxi driver hates injured himself
4. the pilot that the assistant loves hurt themselves

• **Reflexive Anaphora: (Singular/Plural Pronoun) Dataset:** 2500 (Train), 200 (Validation), 200 (Test)

Singular

1. the customer that the ministers hate congratulated herself
2. the surgeons that the dancers like embarrassed himself
3. the authors that the taxi driver hates embarrassed himself
4. the author that the architect admires doubted themselves

Plural

1. the officer that the skaters admire embarrassed themselves
2. the senator that the guard likes embarrassed themselves
3. the customer that the ministers love doubted themselves
4. the managers that the guard admires injured herself

• **Reflexive Anaphora: Test (Singular/Plural Antecedent) Dataset:** 200 (Validation), 200 (Test)

Singular

1. the customer that the skater admires hurt herself
2. the consultant that the executive loves disguised herself
3. the manager that the skaters like embarrassed herself
4. the senators that the guard admires injured himself

Plural

1. the senators that the architects like embarrassed themselves
2. the authors that the executives admire disguised themselves
3. the surgeons that the taxi driver admires doubted themselves
4. the officer that the parents like congratulated themselves

• **Reflexive Anaphora: Test (Singular/Plural Pronoun) Dataset:** 200 (Validation), 200 (Test)

Singular

1. the pilot that the chefs hate hurt himself
2. the teacher that the taxi drivers love hated herself
3. the senator that the assistant loves embarrassed herself
4. the pilot that the skaters admire embarrassed themselves

Plural

1. the authors that the parents admire congratulated themselves
2. the pilots that the chef hates hurt themselves
3. the authors that the parents like congratulated themselves
4. the farmers that the ministers admire injured herself

G. Vision Pretraining Details

We pretrain a Resnet50 model and MLP using SimCLR, a contrastive self-supervised learning algorithm (Chen et al., 2020). This algorithm generates two views of an image using random data augmentations, then maximizes the agreement between representations of these views using a contrastive loss function. We use a temperature of 0.07 for this loss.

Our data augmentations include horizontal flips, affine transformations, color jitters, rotations, and grayscaling. We train for 100 epochs, using a learning rate of .0005 (which is decayed according to a cosine annealing schedule) and a batch size of 256. Images are drawn randomly from the three compositional training sets (**Inside-Contact**, **Number-Contact**, **Inside-Number**). For every rule-following image that is selected, a rule-breaking image from that same dataset is also selected.

We evaluate the Top-5 Accuracy on a held-out validation set after every epoch, and save the weights of the best performing model. Following Chen et al. (2020), we discard the MLP after pretraining, only using the Resnet50 weights to initialize our pretrained models in Section 8. From Figure 16, it is clear that the model converged during training.

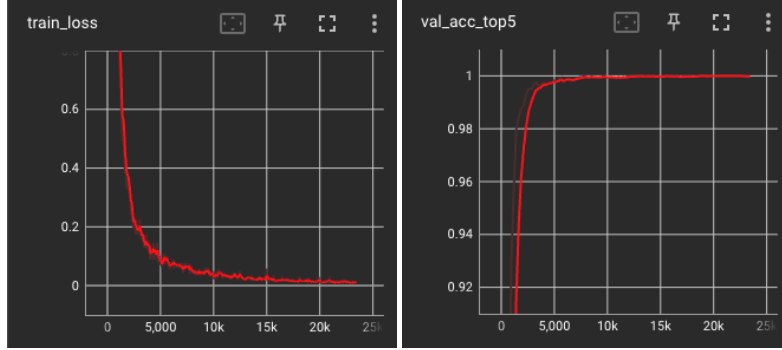


Figure 16. SimCLR Training Graphs. Training Loss (Left), Top-5 Accuracy on a held-out validation set (Right)

We adapted the implementation found in Lippe (2022) to implement SimCLR pretraining.

H. Subnetwork Sparsity Data

In this section, we provide the raw sparsity statistics for each subnetwork trained in this paper. For every subnetwork, we indicate what stage we started masking (0, 3, or 4), provide the number of active parameters in the subnetwork (i.e. the number of 1's in the binary mask), and include the total number of parameters that we mask over (i.e. the number of entries in the binary mask), which is determined by the mask stage.

I. Control Experiment: Random Models

Recent work has demonstrated several surprising properties of masks trained on randomly-initialized networks (Ramanujan et al., 2020; Zhou et al., 2019; Wortsman et al., 2020). One might wonder whether the results demonstrated here could be

TASK	SUBROUTINE	MODEL #	MASK #	MASK STAGE	ACTIVE PARAMETERS	TOTAL PARAMETERS
NUMBER-CONTACT	CONTACT	1	1	4	8059720	19398656
NUMBER-CONTACT	CONTACT	1	2	4	8200381	19398656
NUMBER-CONTACT	CONTACT	1	3	4	8199621	19398656
NUMBER-CONTACT	NUMBER	1	1	0	259611	27911360
NUMBER-CONTACT	NUMBER	1	2	0	264197	27911360
NUMBER-CONTACT	NUMBER	1	3	0	438332	27911360
NUMBER-CONTACT	CONTACT	2	1	3	996278	26476544
NUMBER-CONTACT	CONTACT	2	2	3	1010779	26476544
NUMBER-CONTACT	CONTACT	2	3	3	970624	26476544
NUMBER-CONTACT	NUMBER	2	1	4	1831379	19398656
NUMBER-CONTACT	NUMBER	2	2	4	1822564	19398656
NUMBER-CONTACT	NUMBER	2	3	4	1814451	19398656
NUMBER-CONTACT	CONTACT	3	1	4	6044544	19398656
NUMBER-CONTACT	CONTACT	3	2	4	6111795	19398656
NUMBER-CONTACT	CONTACT	3	3	4	6258924	19398656
NUMBER-CONTACT	NUMBER	3	1	0	225866	27911360
NUMBER-CONTACT	NUMBER	3	2	0	685279	27911360
NUMBER-CONTACT	NUMBER	3	3	0	219003	27911360
INSIDE-CONTACT	INSIDE	1	1	4	2418223	19398656
INSIDE-CONTACT	INSIDE	1	2	4	2384556	19398656
INSIDE-CONTACT	INSIDE	1	3	4	2307045	19398656
INSIDE-CONTACT	CONTACT	1	1	4	1029149	19398656
INSIDE-CONTACT	CONTACT	1	2	4	1057758	19398656
INSIDE-CONTACT	CONTACT	1	3	4	938794	19398656
INSIDE-CONTACT	INSIDE	2	1	3	189266	26476544
INSIDE-CONTACT	INSIDE	2	2	3	140762	26476544
INSIDE-CONTACT	INSIDE	2	3	3	184485	26476544
INSIDE-CONTACT	CONTACT	2	1	3	1266369	26476544
INSIDE-CONTACT	CONTACT	2	2	3	1333968	26476544
INSIDE-CONTACT	CONTACT	2	3	3	1078198	26476544
INSIDE-CONTACT	INSIDE	3	1	3	94253	26476544
INSIDE-CONTACT	INSIDE	3	2	3	159807	26476544
INSIDE-CONTACT	INSIDE	3	3	3	231113	26476544
INSIDE-CONTACT	CONTACT	3	1	3	1681559	26476544
INSIDE-CONTACT	CONTACT	3	2	3	1684466	26476544
INSIDE-CONTACT	CONTACT	3	3	3	1682888	26476544
INSIDE-NUMBER	INSIDE	1	1	4	7004974	19398656
INSIDE-NUMBER	INSIDE	1	2	4	7077554	19398656
INSIDE-NUMBER	INSIDE	1	3	4	7077890	19398656
INSIDE-NUMBER	NUMBER	1	1	3	3190833	26476544
INSIDE-NUMBER	NUMBER	1	2	3	3291780	26476544
INSIDE-NUMBER	NUMBER	1	3	3	3559092	26476544
INSIDE-NUMBER	INSIDE	2	1	4	5255315	19398656
INSIDE-NUMBER	INSIDE	2	2	4	5253035	19398656
INSIDE-NUMBER	INSIDE	2	3	4	5151024	19398656
INSIDE-NUMBER	NUMBER	2	1	4	3149872	19398656
INSIDE-NUMBER	NUMBER	2	2	4	2765010	19398656
INSIDE-NUMBER	NUMBER	2	3	4	2675994	19398656
INSIDE-NUMBER	INSIDE	3	1	3	920241	26476544
INSIDE-NUMBER	INSIDE	3	2	3	853147	26476544
INSIDE-NUMBER	INSIDE	3	3	3	974109	26476544
INSIDE-NUMBER	NUMBER	3	1	4	5046083	19398656
INSIDE-NUMBER	NUMBER	3	2	4	5033831	19398656
INSIDE-NUMBER	NUMBER	3	3	4	5086233	19398656

Table 4. Resnet50 subnetwork sparsity statistics

TASK	SUBROUTINE	MODEL #	MASK #	MASK STAGE	ACTIVE PARAMETERS	TOTAL PARAMETERS
NUMBER-CONTACT	CONTACT	1	1	3	1184224	26476544
NUMBER-CONTACT	CONTACT	1	2	3	875632	26476544
NUMBER-CONTACT	CONTACT	1	3	3	960475	26476544
NUMBER-CONTACT	NUMBER	1	1	4	703485	19398656
NUMBER-CONTACT	NUMBER	1	2	4	682724	19398656
NUMBER-CONTACT	NUMBER	1	3	4	684961	19398656
NUMBER-CONTACT	CONTACT	2	1	3	833083	26476544
NUMBER-CONTACT	CONTACT	2	2	3	935644	26476544
NUMBER-CONTACT	CONTACT	2	3	3	903822	26476544
NUMBER-CONTACT	NUMBER	2	1	4	682249	19398656
NUMBER-CONTACT	NUMBER	2	2	4	660732	19398656
NUMBER-CONTACT	NUMBER	2	3	4	611524	19398656
NUMBER-CONTACT	CONTACT	3	1	3	898919	26476544
NUMBER-CONTACT	CONTACT	3	2	3	1129741	26476544
NUMBER-CONTACT	CONTACT	3	3	3	765665	26476544
NUMBER-CONTACT	NUMBER	3	1	4	8734131	19398656
NUMBER-CONTACT	NUMBER	3	2	4	8880893	19398656
NUMBER-CONTACT	NUMBER	3	3	4	8900554	19398656
INSIDE-CONTACT	INSIDE	1	1	4	138289	19398656
INSIDE-CONTACT	INSIDE	1	2	4	102788	19398656
INSIDE-CONTACT	INSIDE	1	3	4	64056	19398656
INSIDE-CONTACT	CONTACT	1	1	4	687037	19398656
INSIDE-CONTACT	CONTACT	1	2	4	730767	19398656
INSIDE-CONTACT	CONTACT	1	3	4	594200	19398656
INSIDE-CONTACT	INSIDE	2	1	4	119585	19398656
INSIDE-CONTACT	INSIDE	2	2	4	153621	19398656
INSIDE-CONTACT	INSIDE	2	3	4	141847	19398656
INSIDE-CONTACT	CONTACT	2	1	4	880968	19398656
INSIDE-CONTACT	CONTACT	2	2	4	582672	19398656
INSIDE-CONTACT	CONTACT	2	3	4	549542	19398656
INSIDE-CONTACT	INSIDE	3	1	4	444801	19398656
INSIDE-CONTACT	INSIDE	3	2	4	404687	19398656
INSIDE-CONTACT	INSIDE	3	3	4	388647	19398656
INSIDE-CONTACT	CONTACT	3	1	4	2726236	19398656
INSIDE-CONTACT	CONTACT	3	2	4	2712782	19398656
INSIDE-CONTACT	CONTACT	3	3	4	2704681	19398656
INSIDE-NUMBER	INSIDE	1	1	3	811096	26476544
INSIDE-NUMBER	INSIDE	1	2	3	849964	26476544
INSIDE-NUMBER	INSIDE	1	3	3	781551	26476544
INSIDE-NUMBER	NUMBER	1	1	0	14878394	27911360
INSIDE-NUMBER	NUMBER	1	2	0	14739139	27911360
INSIDE-NUMBER	NUMBER	1	3	0	14919954	27911360
INSIDE-NUMBER	INSIDE	2	1	4	375073	19398656
INSIDE-NUMBER	INSIDE	2	2	4	306550	19398656
INSIDE-NUMBER	INSIDE	2	3	4	314610	19398656
INSIDE-NUMBER	NUMBER	2	1	3	2468331	26476544
INSIDE-NUMBER	NUMBER	2	2	3	3106382	26476544
INSIDE-NUMBER	NUMBER	2	3	3	3122791	26476544
INSIDE-NUMBER	INSIDE	3	1	0	660344	27911360
INSIDE-NUMBER	INSIDE	3	2	0	714676	27911360
INSIDE-NUMBER	INSIDE	3	3	0	692889	27911360
INSIDE-NUMBER	NUMBER	3	1	3	3369673	26476544
INSIDE-NUMBER	NUMBER	3	2	3	3661479	26476544
INSIDE-NUMBER	NUMBER	3	3	3	3278225	26476544

Table 5. Resnet50 + SimCLR Subnetwork sparsity statistics

TASK	SUBROUTINE	MODEL #	MASK #	MASK STAGE	ACTIVE PARAMETERS	TOTAL PARAMETERS
NUMBER-CONTACT	CONTACT	1	1	4	12415313	46399488
NUMBER-CONTACT	CONTACT	1	2	4	11886093	46399488
NUMBER-CONTACT	CONTACT	1	3	4	11994752	46399488
NUMBER-CONTACT	NUMBER	1	1	0	364048	71222464
NUMBER-CONTACT	NUMBER	1	2	0	356776	71222464
NUMBER-CONTACT	NUMBER	1	3	0	430018	71222464
NUMBER-CONTACT	CONTACT	2	1	4	8156499	46399488
NUMBER-CONTACT	CONTACT	2	2	4	8188321	46399488
NUMBER-CONTACT	CONTACT	2	3	4	8730014	46399488
NUMBER-CONTACT	NUMBER	2	1	0	489546	71222464
NUMBER-CONTACT	NUMBER	2	2	0	479722	71222464
NUMBER-CONTACT	NUMBER	2	3	0	405563	71222464
NUMBER-CONTACT	CONTACT	3	1	4	11238193	46399488
NUMBER-CONTACT	CONTACT	3	2	4	11246123	46399488
NUMBER-CONTACT	CONTACT	3	3	4	11084672	46399488
NUMBER-CONTACT	NUMBER	3	1	4	792483	46399488
NUMBER-CONTACT	NUMBER	3	2	4	681226	46399488
NUMBER-CONTACT	NUMBER	3	3	4	834326	46399488
INSIDE-CONTACT	INSIDE	1	1	3	177339	67108864
INSIDE-CONTACT	INSIDE	1	2	3	147071	67108864
INSIDE-CONTACT	INSIDE	1	3	3	232306	67108864
INSIDE-CONTACT	CONTACT	1	1	3	1100205	67108864
INSIDE-CONTACT	CONTACT	1	2	3	966156	67108864
INSIDE-CONTACT	CONTACT	1	3	3	1043718	67108864
INSIDE-CONTACT	INSIDE	2	1	0	875532	71222464
INSIDE-CONTACT	INSIDE	2	2	0	493009	71222464
INSIDE-CONTACT	INSIDE	2	3	0	619362	71222464
INSIDE-CONTACT	CONTACT	2	1	3	5898635	67108864
INSIDE-CONTACT	CONTACT	2	2	3	6213208	67108864
INSIDE-CONTACT	CONTACT	2	3	3	5909038	67108864
INSIDE-CONTACT	INSIDE	3	1	3	557265	67108864
INSIDE-CONTACT	INSIDE	3	2	3	330289	67108864
INSIDE-CONTACT	INSIDE	3	3	3	710769	67108864
INSIDE-CONTACT	CONTACT	3	1	3	4632439	67108864
INSIDE-CONTACT	CONTACT	3	2	3	4376935	67108864
INSIDE-CONTACT	CONTACT	3	3	3	4964646	67108864
INSIDE-NUMBER	INSIDE	1	1	3	2081068	67108864
INSIDE-NUMBER	INSIDE	1	2	3	2106222	67108864
INSIDE-NUMBER	INSIDE	1	3	3	2007091	67108864
INSIDE-NUMBER	NUMBER	1	1	4	3541726	46399488
INSIDE-NUMBER	NUMBER	1	2	4	3560812	46399488
INSIDE-NUMBER	NUMBER	1	3	4	3583605	46399488
INSIDE-NUMBER	INSIDE	2	1	0	2242819	71222464
INSIDE-NUMBER	INSIDE	2	2	0	1963701	71222464
INSIDE-NUMBER	INSIDE	2	3	0	1330134	71222464
INSIDE-NUMBER	NUMBER	2	1	3	5749408	67108864
INSIDE-NUMBER	NUMBER	2	2	3	5511381	67108864
INSIDE-NUMBER	NUMBER	2	3	3	5472792	67108864
INSIDE-NUMBER	INSIDE	3	1	0	808884	71222464
INSIDE-NUMBER	INSIDE	3	2	0	851288	71222464
INSIDE-NUMBER	INSIDE	3	3	0	731729	71222464
INSIDE-NUMBER	NUMBER	3	1	0	3487441	71222464
INSIDE-NUMBER	NUMBER	3	2	0	3528010	71222464
INSIDE-NUMBER	NUMBER	3	3	0	4330284	71222464

Table 6. Wide Resnet50 Subnetwork sparsity statistics

TASK	SUBROUTINE	MODEL #	MASK #	MASK STAGE	ACTIVE PARAMETERS	TOTAL PARAMETERS
(S) SV AGREEMENT	SUBJECT	1	1	0	1246922	12845056
(S) SV AGREEMENT	SUBJECT	1	2	0	1242347	12845056
(S) SV AGREEMENT	SUBJECT	1	3	0	2128824	12845056
(S) SV AGREEMENT	VERB	1	1	0	1668369	12845056
(S) SV AGREEMENT	VERB	1	2	0	2600240	12845056
(S) SV AGREEMENT	VERB	1	3	0	3353398	12845056
(S) SV AGREEMENT	SUBJECT	2	1	0	2728632	12845056
(S) SV AGREEMENT	SUBJECT	2	2	0	2663842	12845056
(S) SV AGREEMENT	SUBJECT	2	3	0	2681724	12845056
(S) SV AGREEMENT	VERB	2	1	0	951132	12845056
(S) SV AGREEMENT	VERB	2	2	0	1044003	12845056
(S) SV AGREEMENT	VERB	2	3	0	1084848	12845056
(S) SV AGREEMENT	SUBJECT	3	1	0	328484	12845056
(S) SV AGREEMENT	SUBJECT	3	2	0	720899	12845056
(S) SV AGREEMENT	SUBJECT	3	3	0	323764	12845056
(S) SV AGREEMENT	VERB	3	1	3	1794939	6553600
(S) SV AGREEMENT	VERB	3	2	3	1702597	6553600
(S) SV AGREEMENT	VERB	3	3	3	1567156	6553600
(P) SV AGREEMENT	SUBJECT	1	1	0	69748	12845056
(P) SV AGREEMENT	SUBJECT	1	2	0	68641	12845056
(P) SV AGREEMENT	SUBJECT	1	3	0	52336	12845056
(P) SV AGREEMENT	VERB	1	1	3	640889	6553600
(P) SV AGREEMENT	VERB	1	2	3	477101	6553600
(P) SV AGREEMENT	VERB	1	3	3	656202	6553600
(P) SV AGREEMENT	SUBJECT	2	1	0	119037	12845056
(P) SV AGREEMENT	SUBJECT	2	2	0	125594	12845056
(P) SV AGREEMENT	SUBJECT	2	3	0	122828	12845056
(P) SV AGREEMENT	VERB	2	1	0	215555	12845056
(P) SV AGREEMENT	VERB	2	2	0	202185	12845056
(P) SV AGREEMENT	VERB	2	3	0	56134	12845056
(P) SV AGREEMENT	SUBJECT	3	1	0	86084	12845056
(P) SV AGREEMENT	SUBJECT	3	2	0	49694	12845056
(P) SV AGREEMENT	SUBJECT	3	3	0	166614	12845056
(P) SV AGREEMENT	VERB	3	1	0	149398	12845056
(P) SV AGREEMENT	VERB	3	2	0	221074	12845056
(P) SV AGREEMENT	VERB	3	3	0	133149	12845056

Table 7. BERT Subject-Verb Agreement Subnetwork sparsity statistics

TASK	SUBROUTINE	MODEL #	MASK #	MASK STAGE	ACTIVE PARAMETERS	TOTAL PARAMETERS
(S) ANAPHORA	PRONOUN	1	1	0	370568	12845056
(S) ANAPHORA	PRONOUN	1	2	0	372203	12845056
(S) ANAPHORA	PRONOUN	1	3	0	369123	12845056
(S) ANAPHORA	ANTECEDENT	1	1	0	169120	12845056
(S) ANAPHORA	ANTECEDENT	1	2	0	150554	12845056
(S) ANAPHORA	ANTECEDENT	1	3	0	231819	12845056
(S) ANAPHORA	PRONOUN	2	1	0	968021	12845056
(S) ANAPHORA	PRONOUN	2	2	0	971063	12845056
(S) ANAPHORA	PRONOUN	2	3	0	970910	12845056
(S) ANAPHORA	ANTECEDENT	2	1	0	108544	12845056
(S) ANAPHORA	ANTECEDENT	2	2	0	110871	12845056
(S) ANAPHORA	ANTECEDENT	2	3	0	108347	12845056
(S) ANAPHORA	PRONOUN	3	1	0	79069	12845056
(S) ANAPHORA	PRONOUN	3	2	0	79031	12845056
(S) ANAPHORA	PRONOUN	3	3	0	82788	12845056
(S) ANAPHORA	ANTECEDENT	3	1	0	1854552	12845056
(S) ANAPHORA	ANTECEDENT	3	2	0	1848327	12845056
(S) ANAPHORA	ANTECEDENT	3	3	0	1874968	12845056
(P) ANAPHORA	PRONOUN	1	1	0	325597	12845056
(P) ANAPHORA	PRONOUN	1	2	0	417498	12845056
(P) ANAPHORA	PRONOUN	1	3	0	642805	12845056
(P) ANAPHORA	ANTECEDENT	1	1	0	286739	12845056
(P) ANAPHORA	ANTECEDENT	1	2	0	336572	12845056
(P) ANAPHORA	ANTECEDENT	1	3	0	405887	12845056
(P) ANAPHORA	PRONOUN	2	1	0	24818	12845056
(P) ANAPHORA	PRONOUN	2	2	0	24805	12845056
(P) ANAPHORA	PRONOUN	2	3	0	24855	12845056
(P) ANAPHORA	ANTECEDENT	2	1	3	1154161	6553600
(P) ANAPHORA	ANTECEDENT	2	2	3	1183436	6553600
(P) ANAPHORA	ANTECEDENT	2	3	3	1159462	6553600
(P) ANAPHORA	PRONOUN	3	1	0	144186	12845056
(P) ANAPHORA	PRONOUN	3	2	0	151531	12845056
(P) ANAPHORA	PRONOUN	3	3	0	153897	12845056
(P) ANAPHORA	ANTECEDENT	3	1	0	4606842	12845056
(P) ANAPHORA	ANTECEDENT	3	2	0	5134758	12845056
(P) ANAPHORA	ANTECEDENT	3	3	0	5041888	12845056

Table 8. BERT Anaphora Subnetwork sparsity statistics

TASK	SUBROUTINE	MODEL #	MASK #	MASK STAGE	ACTIVE PARAMETERS	TOTAL PARAMETERS
(S) SV AGREEMENT	SUBJECT	1	1	0	59736	12845056
(S) SV AGREEMENT	SUBJECT	1	2	0	839770	12845056
(S) SV AGREEMENT	SUBJECT	1	3	0	620869	12845056
(S) SV AGREEMENT	VERB	1	1	3	65229	6553600
(S) SV AGREEMENT	VERB	1	2	3	65356	6553600
(S) SV AGREEMENT	VERB	1	3	3	65220	6553600
(S) SV AGREEMENT	SUBJECT	2	1	0	511359	12845056
(S) SV AGREEMENT	SUBJECT	2	2	0	70725	12845056
(S) SV AGREEMENT	SUBJECT	2	3	0	555174	12845056
(S) SV AGREEMENT	VERB	2	1	0	16940	12845056
(S) SV AGREEMENT	VERB	2	2	0	39218	12845056
(S) SV AGREEMENT	VERB	2	3	0	19321	12845056
(S) SV AGREEMENT	SUBJECT	3	1	0	8514	12845056
(S) SV AGREEMENT	SUBJECT	3	2	0	8613	12845056
(S) SV AGREEMENT	SUBJECT	3	3	0	8593	12845056
(S) SV AGREEMENT	VERB	3	1	3	64969	6553600
(S) SV AGREEMENT	VERB	3	2	3	65098	6553600
(S) SV AGREEMENT	VERB	3	3	3	64955	6553600
(P) SV AGREEMENT	SUBJECT	1	1	0	45792	12845056
(P) SV AGREEMENT	SUBJECT	1	2	0	45527	12845056
(P) SV AGREEMENT	SUBJECT	1	3	0	45616	12845056
(P) SV AGREEMENT	VERB	1	1	0	16800	12845056
(P) SV AGREEMENT	VERB	1	2	0	24013	12845056
(P) SV AGREEMENT	VERB	1	3	0	23988	12845056
(P) SV AGREEMENT	SUBJECT	2	1	0	47651	12845056
(P) SV AGREEMENT	SUBJECT	2	2	0	47502	12845056
(P) SV AGREEMENT	SUBJECT	2	3	0	47811	12845056
(P) SV AGREEMENT	VERB	2	1	3	100005	6553600
(P) SV AGREEMENT	VERB	2	2	3	100100	6553600
(P) SV AGREEMENT	VERB	2	3	3	100029	6553600
(P) SV AGREEMENT	SUBJECT	3	1	3	81133	6553600
(P) SV AGREEMENT	SUBJECT	3	2	3	81203	6553600
(P) SV AGREEMENT	SUBJECT	3	3	3	81218	6553600
(P) SV AGREEMENT	VERB	3	1	0	15302	12845056
(P) SV AGREEMENT	VERB	3	2	0	9423	12845056
(P) SV AGREEMENT	VERB	3	3	0	15900	12845056

Table 9. BERT + LM Subject-Verb Agreement Subnetwork sparsity statistics

TASK	SUBROUTINE	MODEL #	MASK #	MASK STAGE	ACTIVE PARAMETERS	TOTAL PARAMETERS
(S) ANAPHORA	PRONOUN	1	1	0	6590452	12845056
(S) ANAPHORA	PRONOUN	1	2	0	6702195	12845056
(S) ANAPHORA	PRONOUN	1	3	0	6519670	12845056
(S) ANAPHORA	ANTECEDENT	1	1	0	832044	12845056
(S) ANAPHORA	ANTECEDENT	1	2	0	833149	12845056
(S) ANAPHORA	ANTECEDENT	1	3	0	835278	12845056
(S) ANAPHORA	PRONOUN	2	1	3	193677	6553600
(S) ANAPHORA	PRONOUN	2	2	3	198612	6553600
(S) ANAPHORA	PRONOUN	2	3	3	198956	6553600
(S) ANAPHORA	ANTECEDENT	2	1	0	39355	12845056
(S) ANAPHORA	ANTECEDENT	2	2	0	27784	12845056
(S) ANAPHORA	ANTECEDENT	2	3	0	34674	12845056
(S) ANAPHORA	PRONOUN	3	1	0	36495	12845056
(S) ANAPHORA	PRONOUN	3	2	0	1458843	12845056
(S) ANAPHORA	PRONOUN	3	3	0	75100	12845056
(S) ANAPHORA	ANTECEDENT	3	1	0	648936	12845056
(S) ANAPHORA	ANTECEDENT	3	2	0	680218	12845056
(S) ANAPHORA	ANTECEDENT	3	3	0	760770	12845056
(P) ANAPHORA	PRONOUN	1	1	0	11374	12845056
(P) ANAPHORA	PRONOUN	1	2	0	11251	12845056
(P) ANAPHORA	PRONOUN	1	3	0	11369	12845056
(P) ANAPHORA	ANTECEDENT	1	1	0	1152444	12845056
(P) ANAPHORA	ANTECEDENT	1	2	0	1152518	12845056
(P) ANAPHORA	ANTECEDENT	1	3	0	1149693	12845056
(P) ANAPHORA	PRONOUN	2	1	0	11327	12845056
(P) ANAPHORA	PRONOUN	2	2	0	11321	12845056
(P) ANAPHORA	PRONOUN	2	3	0	11275	12845056
(P) ANAPHORA	ANTECEDENT	2	1	0	43274	12845056
(P) ANAPHORA	ANTECEDENT	2	2	0	44220	12845056
(P) ANAPHORA	ANTECEDENT	2	3	0	45632	12845056
(P) ANAPHORA	PRONOUN	3	1	0	28866	12845056
(P) ANAPHORA	PRONOUN	3	2	0	28887	12845056
(P) ANAPHORA	PRONOUN	3	3	0	29101	12845056
(P) ANAPHORA	ANTECEDENT	3	1	0	4292104	12845056
(P) ANAPHORA	ANTECEDENT	3	2	0	4350952	12845056
(P) ANAPHORA	ANTECEDENT	3	3	0	4048117	12845056

Table 10. BERT + LM Anaphora Subnetwork sparsity statistics

obtained by training a binary mask over randomly-initialized network. If so, this would pose a serious problem for our interpretation of the data: producing the same results in a randomly-initialized network would decouple the behavior of the discovered subnetworks from the representations learned by the underlying base model.

We carry out this experiment as a control. Specifically, we run the exact same mask training procedure used to generate the results in Section 7, except we use randomly-initialized models rather than models trained on compositional tasks. In Section 7, each (model, subroutine) pair had its own set of masking hyperparameters. We use these same hyperparameters for each (randomly-initialized model, subroutine) pair in order to make the results as comparable as possible.

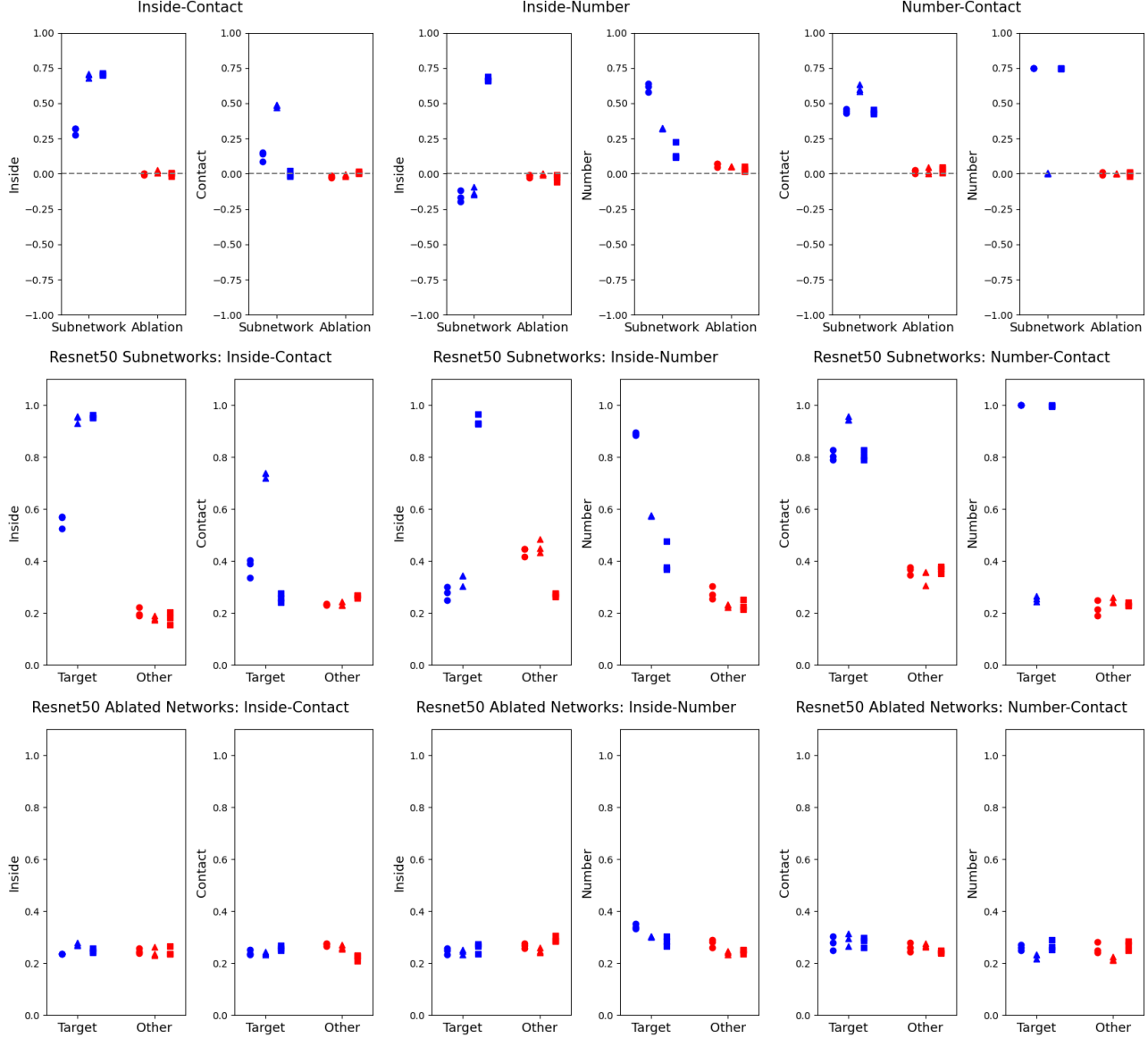


Figure 17. Results from training masks over a randomly-initialized Resnet50. (Top) Plots displaying differences in performance. (Middle) Plots displaying subnetwork performance on each task. (Bottom) Plots displaying ablated model performance on each task. Across the board, we see that masks over random networks can produce subnetworks that achieve better accuracy on on **Test Target Subroutine** than on **Test Other Subroutine**, but that ablating these subnetworks results in (equally) poor performance on both of these datasets.

In Figure 17 and 18, we observe that masking random networks produces distinctly different patterns of results than we presented in Section 7. Though it is possible find a subnetwork that computes a target subroutine and not the other subroutine,

the ablation results do not follow the pattern that one would expect of a compositional model. This accords with [Ramanujan et al. \(2020\)](#), which demonstrates that training a binary mask over a randomly-weighted network can still produce performant subnetworks. The ablation results indicate that these subnetworks are not causally implicated in model behavior. In the case of Resnet50 (Figure 17, Bottom) we observe that ablating the learned subnetworks collapses performance to chance for all tasks. In the case of BERT Small (Figure 18, Bottom), we observe that ablating the learned subnetworks oftentimes yields high performance on **Test Target Subroutine** and low performance on **Test Other Subroutine**, which is the *opposite* of the expected trend for a compositional model. Thus, we can be more confident that the main results presented in Section 7 reflect the internal mechanisms of trained models, and are not epiphenomenal artifacts of training binary masks over networks.

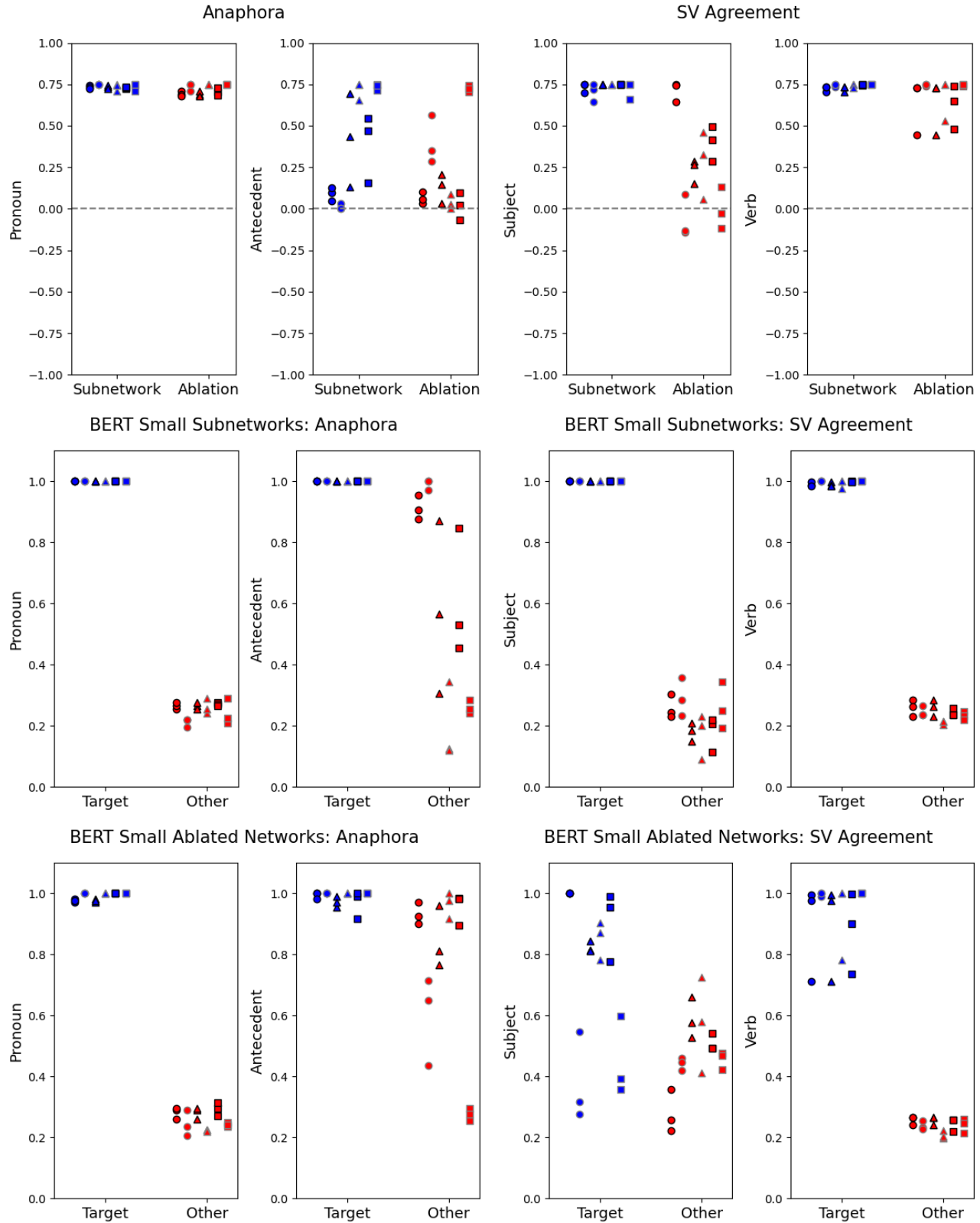


Figure 18. Results from training masks over a randomly-initialized BERT Small. (Top) Plots displaying differences in performance. (Middle) Plots displaying subnetwork performance on each task. (Bottom) Plots displaying ablated model performance on each task. Across the board, we see that masks over random networks can produce subnetworks that achieve better accuracy on on **Test Target Subroutine** than on **Test Other Subroutine**. Surprisingly, ablating these subnetworks still results in better accuracy on on **Test Target Subroutine** than on **Test Other Subroutine**.